EurJIC

European Journal of Inorganic Chemistry

Chemistry Europe

European Chemical Societies Publishing

Accepted Article

Title: Structure and reactivity of NO/NO+/NO– pincer and porphyrin complexes

Authors: Cecilia Mariel Gallego, Agostina Mazzeo, Carina Gaviglio, Juan Pellegrino, and Fabio Doctorovich

To be cited as: *Eur. J. Inorg. Chem.* 10.1002/ejic.202100682

Link to VoR: https://doi.org/10.1002/ejic.202100682

WILEY-VCH

WILEY-VCH

REVIEW

Structure and reactivity of NO/NO+/NO- pincer and porphyrin complexes

Cecilia Mariel Gallego†[a], Agostina Mazzeo†[a], Carina Gaviglio[b], Juan Pellegrino*[a] and Fabio Doctorovich*[a]

[a] Prof. Dr. F. Doctorovich, Dr. J. Pellegrino, A. Mazzeo, C.M. Gallego
Departamento de Química Inorgánica, Analítica y Química Física
Facultad de Ciencias Exactas y Naturales, Universidad de Buenos Aires
Pabellón 2, Ciudad Universitaria, Buenos Aires, Argentina
E-mail: pellegrino@qi.fcen.uba.ar, doctorovich@qi.fcen.uba.ar
[b] Dr. C. Gaviglio
Departamento de Física de la Materia Condensada
Comisión Nacional de Energía Atómica, CAC-GIyANN
Avenida General Paz 1499, San Martín, Buenos Aires, Argentina
†These authors contributed equally.

Abstract: This review covers recent progress in the field of nitrosyl pincer and porphyrinate complexes, and how their reactivity depends on the redox state of the NO ligand. Synthetic methods, and the most significant structural information, spectroelectrochemical studies, and different reactivities of nitrosyl pincer complexes are presented. These include selective activation and functionalization of carbon-halogen bonds, catalysis for a variety of specific organic reactions, mediation of NO disproportionation and reversible coordination of solvents and weakly-coordinating anions. Regarding the porphyrinate complexes, the focus is on biorelevant nitroxyl (NO^-/HNO) complexes, discussing pioneering studies along with preparation and common characterization methods. Their relative stability in different conditions is compared, and possible decomposition mechanisms are discussed in terms of their ability to act as biomimetic models for enzymatic systems.

M.Sc. Cecilia M. Gallego was born in 1993 in Buenos Aires, Argentina. She works as a teaching assistant in the University of Buenos Aires, where she graduated from her M.Sc. degree, and where she now works in her Ph.D. thesis exploring the combined effect of nitric oxide and pincer ligands in coordination chemistry, supervised by Dr. Pellegrino and Prof. Doctorovich.

M.Sc. Agostina M. Mazzeo was born in Buenos Aires, Argentina, in 1991. She obtained her M.Sc. in Chemistry from the University of Buenos Aires in 2015, where she works as a teaching assistant. She is currently completing her Ph.D. thesis focused on organometallic and bioinorganic chemistry of iron NO and HNO porphyrin complexes under the supervision of Dr. Pellegrino and Prof. Doctorovich.

Dr. Carina Gaviglio is an assistant researcher at CONICET, Argentina. She obtained her M. Sc. in Chemistry from the National University of Litoral and her Ph. D. in Chemistry from University of Buenos Aires, both in Argentina. Her PhD thesis focused on organometallic chemistry and included a one-year stay at the Weizmann Institute of Science, and she afterwards accomplished a postdoc in electrochemistry. She has been involved in several research projects including organometallic chemistry, electrochemistry and sensor applications. Nowadays her main research interests include Organometallic pincer complexes, Crystallography and Phase Transitions in metal complexes.

Dr. Juan Pellegrino received his Ph.D. in Chemistry in 2013 at University of Buenos Aires. His doctoral thesis has focused on organometallic and bioinorganic chemistry of NO complexes. After a postdoc stay at Prof. Milstein's lab at the Weizmann Institute of Science he established as an assistant researcher at University of Buenos Aires. His main research interests include the use of transition metal complexes with non-innocent ligands in key chemical transformations, such as bond activation or proton reduction.

Prof. Dr. Fabio Doctorovich, Full Professor at the University of Buenos Aires and Researcher at CONICET, obtained his PhD in Organic Chemistry from the University of Buenos Aires in 1990 He was a postdoctoral fellow at the Georgia Institute of Technology working with Prof. E.C. Ashby and K. Barefield, on single electron transfer, and on chemical reactions taking place in nuclear waste tanks. Back in Argentina (UBA), he started to work on nitric oxide (NO), including organic nitrosocompounds, inorganic iron, rhodium, ruthenium and iridium nitrosyl complexes, and reactivity of metalloporphyrins and pincer complexes towards HNO. He also worked on CO complexes, catalytic reactions, and other topics. Nowadays his main research focus is on reactions involving HNO. Prof. Doctorovich has published over 120 works in international journals, and co-edited the book *The Chemistry and Biology of Nitroxyl (HNO)*. He was awarded a Guggenheim Fellowship in 2011.

1. Introduction

Since the discovery of its endogenous formation and its physiological relevance, nitric oxide (NO•) has been widely studied as one of the central actors in the field of bioinorganic chemistry. Its redox non-innocence has also placed it as a useful ligand for organometallic chemistry transformations. Nitric oxide can bind metal centers as NO^+ (nitrosonium), NO• or HNO/NO^- (nitroxyl), which results in ambiguity for the assignation of the oxidation states in M-NO fragments. To circumvent such problems, Enemark and Feltham's notation is generally used.[1] In this notation, the fragments are represented as $\{MNO\}^n$, where *n* is the sum of *d* electrons in the metal and of π^* electrons in NO. Its relevance relies mostly on the fact that it allows rationalization of the MNO geometry (specifically the MNO angle) of a wide range of different complexes. Predictions of MNO angle are then based on the number *n* and the overall geometry of the complex, regardless of the coligands. As an example, Figure 1 shows the XRD structures of the three $\{Fe(OEP)NO\}^n$ porphyrin complexes with n = 6, 7 and 8, highlighting the difference in the MNO angle as a function of *n*.[2–4]

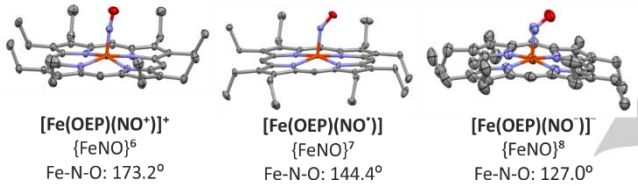

Figure 1. Variation of the Fe-N-O angle for the $\{Fe(OEP)NO\}n$ with n = 6, 7 and 8.

Pincer ligands and porphyrins constitute two representative types of ligands for the organometallic and bioinorganic chemistry of NO and HNO/NO^- respectively, and they both have been the focus of different studies in our research group.

On the one hand, pincer ligands consist of a broad family of tridentate organic ligands with meridional coordination. The arms of the pincer ligands can vary both in length and composition, and usually bind the metal center through neutral groups *E* and *E'*, which may or may not differ. The central binding, *Y*, initially a monoanionic carbon in an aryl system, can be either a neutral or an anionic group. Pincer ligands are usually denoted by the atoms that bind the metal center, as *EYE'*. Figure 2 summarizes the generic scaffold for a pincer ligand indicating the various modifications that their structure may present, which reflects the versatility of the system.

Since the pioneer works of Shaw in 1970-80,[5–8] centered on a variety of PCP-based pincer complexes of Pt, Pd, Ir, Ni and Rh, a consistent growth of studies of these type of systems has been observed in the literature which are still today continually renewed. The structural versatility of pincer ligands has been exploited for several uses, such as catalysis, stabilization of unusual molecules, use as building blocks for self-assembled systems and development of gas sensors.[9–12]

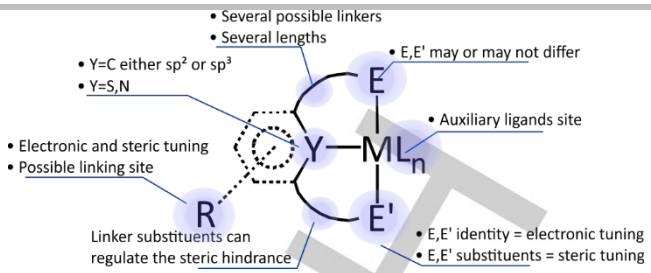

Figure 2. Generic structure for a pincer ligand and its possible modifications.

Such structural diversity as can be seen in Figure 2 also translates into chemical versatility, since pincer ligands can be used to tune both electronic and steric parameters on the metal center. Pincer ligands were initially conceived as purely spectator ligands. However, this conception has been changed in time through reports of different reactions where transformations centered on the pincer ligand allowed different types of reactivities.[10,13] Some of the transformations consist of hemilability of one of the ligand arms,[14–21] formation of C-H agostic interactions,[22] dearomatization of aryl systems,[23] and even reversible collapse of the pincer platform.[24]

However, the broad scope of pincer complexes greatly contrasts with that of pincer nitrosyl complexes, which have comparably been far less consistently studied. Our laboratory group has recently inaugurated a line of research focused on studying the joint effect of pincer ligands' fine-tuning possibilities with nitric oxide's redox versatility. In this review, our studies on $\{RhNO\}^n$ pincer complexes will be described, along with related antecedents.

On the other hand, nitrosyl porphyrin complexes, especially $\{FeNO\}^{6/7/8}$, have been widely studied for the last decades, mainly due to their special relevance as biomimetic models for enzymatic reaction intermediates of the nitrogen cycle, which have been detected and characterized. More recently, the more elusive reduced *nitroxyl* porphyrin complexes, $\{Fe(H)NO\}^8$, have gained researchers' interest, not only because such species have also been proposed as enzymatic intermediates, but also due to the open question regarding the possibility of nitroxyl endogenous formation and action as a biological metabolite. Moreover, the transport of physiologically active nitrogen species (NO•, NO^- and HNO) and their therapeutic effects are closely related to these molecules' interactions with proteins bearing porphyrin active sites, especially of heme nature. In this context, metal-porphyrin platforms prove to be very useful, not only for their structural similarity with naturally occurring protein active sites, but also because they provide a robust scaffold in which highly reactive species such as HNO can be relatively stabilized, allowing further investigation of its chemical properties and reactivity. Figure 3 shows a generic metalloporphyrin structure with a coordinated M^{z+} metal ion, in which the *meso* and β substitution positions are depicted. Our journey in the stabilization of the initially elusive $\{FeNO\}^8$ species in porphyrin platforms will also be addressed in this review, along with the most relevant related literature.

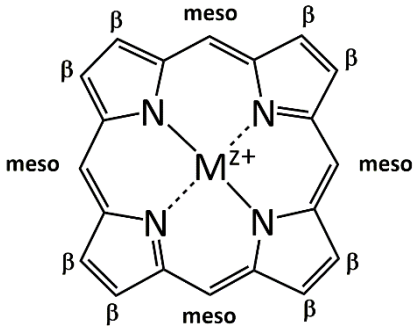

Figure 3. Generic metalloporphyrin structure, showing the usual substitution position and a coordinated metal ion.

2. Pincer nitrosyls

2.1. Structural properties and synthesis

Characterization of pincer nitrosyl complexes is usually comprised of XRD, FTIR and ^{31}P-NMR analysis (the latter on account of most pincer scaffolds being phosphine-based). A summary can be seen in Table 1 (next page). Some useful diagnostic signals should be duly noted. To begin with, FTIR ν(NO) signals are particularly useful when trying to discern a NO^+ from a NO^- configuration, although in cases where stretching frequencies are roughly between 1600 and 1720 cm^{-1} they are insufficient to draw a conclusion, since both linear and bent nitrosyls overlap at these values.

XRD elucidated structures are much more informative, albeit harder to obtain. As a general rule, bent nitrosyl angles are around 120°-130° whereas linear nitrosyls mostly coincide with the expected 180° angle. However, a notable exception to this last remark are the cases where linear NO locates *trans* to the central donor atom of the pincer ligand, where the angles are significantly smaller, as can be seen in complexes **(6$^+$)**, **(9$^+$)** and **(19$^+$)**. This deviation is a result of the strong σ-donation from the aryl ring.[25] There are also some more ambiguous cases, for which the term "*half-bent*" nitrosyls has been coined, where M-N-O angles range from 140°-150°. Caulton's group has studied this intermediate behavior by comparison of a Ni(PNP)(NO) half-bent system **(4)** with linear Ni(PNP)(CO). They found that the conformations of the *t*-Bu groups of the pincer ligand did not differ, and also that the NiNO angle was not affected by exchanging of *t*-Bu for Me and thus discarded a steric origin. Instead, an electronic influence was proposed to be the origin of this type of conformation. DFT calculations of half-bent systems showed large spin densities to be located on the nitrosyl ligand, which could be more reasonably thought of as radical $NO^{\bullet}$ coordinating via a lone pair in the N atom.[26,27]

^{31}P-NMR signals are also greatly useful for phosphine-based pincer ligands, their chemical shift being influenced by the electron density on the metallic center, thus giving indirect evidence of either bent or linear nitrosyls. Another useful probe for nitrosyl configuration in pincer ligands that we have exploited is ^{15}N-NMR.[28,29] In Table 2 it becomes apparent that bent nitrosyls have a large downfield shift when compared to linear nitrosyl configurations. In addition, and differently from what was observed for ^{31}P-NMR, the coupling constant $J(^{103}Rh,^{15}N)$ is also diagnostic of nitrosyl configuration: whereas *sp*-hybridization in linear NO configurations results in doublets, sp^2-hybridization in bent NO configurations presents no coupling whatsoever. ^{15}N-NMR as a probe for nitrosyl ligands therefore bears the advantage of being quite a conclusive tool where two separate parameters with better discerning ranges than FTIR can be used to distinguish bent from linear NO. However, it also bears the disadvantage of requiring enriched ^{15}N samples, which implies a separate synthesis, and hence it is not useful for a quick decision.

Another valid different strategy for discerning MNO configuration involves working with DFT calculations. Kirchner's group has consistently used a DFT analysis on frontier orbitals for a variety of transition metal complexes (some of them illustrated in Table 1). The latter allows them to deduce the number of *d* electrons, thus obtaining the metallic center oxidation state and the overall MNO configuration.[22,30–32] However, it must be noted that the reliability of this strategy depends strongly on the quality of the calculations performed, especially since transition metals can be difficult to model. Therefore, this tool is best applied when complemented by some experimental characterizations.

Table 2. ^{15}N-NMR signals for a series of Rh complexes.

(6$^+$)	**(7)**	**(8^{2+})**	**(9$^+$)**
$Rh^{I}NO^+$	$Rh^{III}NO^-$	$Rh^{III}NO^-$	$Rh^{I}NO^+$
377.88 ppm (d, 35.3 Hz)	841.18 ppm (br s)	829.76 ppm (br s)	377.06 ppm (d, 33.6 Hz)

Synthetic strategies for the preparation of pincer nitrosyl complexes are not greatly varied. Most used is the direct method of nitrosylation by injection of gaseous nitric oxide into a solution of the pincer precursor complex.[22,26,27,30,33–35] This route was first employed by Milstein's group, who proved Rh(PNP)(NO)(Cl) **(1$^+$)** obtention could be achieved both by reaction of a Rh(II) precursor and $NO^{\bullet}$ and by reaction of Rh(I) and NO^+, as is depicted in Scheme 1.[33] This last alternative has been scarcely reported thereafter.[31] A third strategy consists of chelating a complex already bearing an NO ligand with the desired pincer ligand.[36,37]

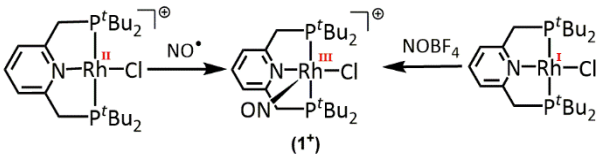

Scheme 1. Obtention of **(1$^+$)** from Rh(II) and $NO^{\bullet}$ and from Rh(I) and NO^+.

Within our group, a PCP ligand was chosen as a first approach to these systems given it is one of the most reported and better-known scaffolds for pincer ligands.[28] Up to that moment, very few pincer nitrosyls had been reported, none with a PCP scaffold.[26,27,33,36] Synthesis consisted of reaction of Rh(PCP)(N_2) with a nitrosonium salt yielding $[Rh(PCP)(NO)]^+$ **(6$^+$)**. This linear nitrosyl complex (*vide infra*) was found to bend by reaction with LiCl. This transformation included binding of a chloride ligand, bending of NO^+ to NO^-, and oxidation of the metal center from Rh(I) to Rh(III), yielding Rh(PCP)(NO)(Cl) **(7)**. This reaction proved to be easily reversed by addition of HBF_4•$O(C_2H_5)_2$, which produced abstraction of the chloride ligand with formation of HCl and **(6$^+$)**. No HNO complex was formed (Scheme 2). Different

pincer ligands were also explored in this first work, namely a PNP and a PC^{CH2}P ligand. Although for PNP the route was analogous to that used for **(6$^+$)**, that is, a Rh(I) complex reacting with NO$^+$, the obtained product was not a Rh(I) one but pentacoordinate Rh(III), [Rh(PNP)(NO)(CH$_3$CN)]$^{2+}$ **(8^{2+})**. As for PC^{CH2}P, a different route was employed, consisting of reaction nitrosylation with NO$^+$ of a Rh(III) precursor (Scheme 3). Interestingly, the reaction involves a multi-step rearrangement which drastically changes the character of the pincer ligand yielding [Rh(PC ^{CH2}P)(NO)]$^+$ **(9$^+$)**.

Table 1. Selected pincer nitrosyl complexes and their relevant structural parameters, ordered chronologically by year of report.

Complex	∠MNO / deg	$\nu_{(NO)}$ / cm^{-1}	^{31}P-NMR	Config.	Ref.	Complex	∠MNO / deg	$\nu_{(NO)}$ / cm^{-1}	^{31}P-NMR	Config.	Ref.
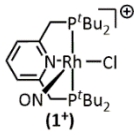 **(1$^+$)**	122.0	1675	67.2 ppm (d, 114 Hz)	Rh^{III}NO$^-$	[33]	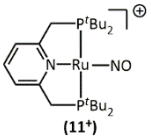 **(11$^+$)**	176.4	1759	80.6 ppm (s)	Ru^{0}NO$^+$	[37]
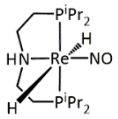 **(2)**	177.7	1679	67.2 ppm (s)	Re^{I}NO$^+$	[36]	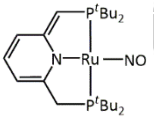 **(12)**	179.6	1916	78.73 and 74.88 ppm (both d, 200 Hz)	Ru^{0}NO$^+$	[37]
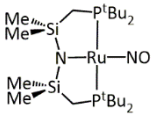 **(3)**	179.2	1691	78.34 ppm (s)	Ru^{0}NO$^+$	[38]	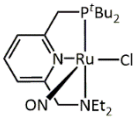 **(13)**	130.2	1679	56.6 ppm	Ru^{II}NO$^-$	[37]
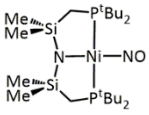 **(4)**	149.3	1654	68.3 ppm (s)	*"half-bent"*	[27]	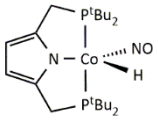 **(14)**	151.7	1609	111.7 ppm (s)	undefined	[35]
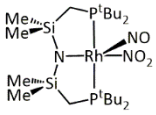 **(5)**	121.1	1677 and 1649	53.7 ppm (d, 119.9 Hz)	Rh^{III}NO$^-$	[26]	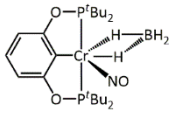 **(15)**	173.4	1654	--	Cr^{I}NO$^+$	[30]
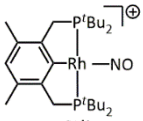 **(6$^+$)**	159.9	1834	104.02 ppm (d, 130.6Hz)	Rh^{I}NO$^+$	[28]	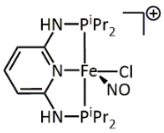 **(16$^+$)**	161.4	1747	--	Fe^{I}NO$^+$	[31]
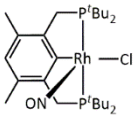 **(7)**	127.4	1618	74.92 ppm (d,143.9 Hz)	Rh^{III}NO$^-$	[28]	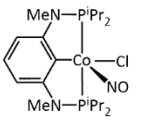 **(17)**	140.1	1643	77.4 ppm (br s)	Co^{III}NO$^-$	[39]
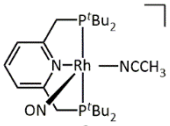 **(8^{2+})**	122.4	1703	73.98 ppm (d, 105.1 Hz)	Rh^{III}NO$^-$	[28]	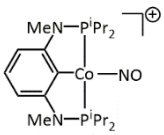 **(18$^+$)**	176.6	1806	156.0 ppm (br s)	Co^{I}NO$^+$	[39]
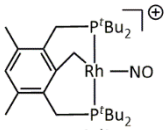 **(9$^+$)**	156.3	1726	109.62 ppm (d, 153.7 Hz)	Rh^{I}NO$^+$	[28]	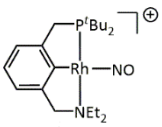 **(19$^+$)**	162.5	1837	109.45 ppm (d, 160.6 Hz)	Rh^{I}NO$^+$	[40]
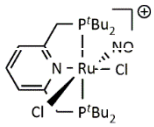 **(10$^+$)**	178.1	1867	66.7 ppm (s)	Ru^{II}NO$^+$	[37]	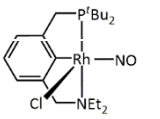 **(20)**	128.6	1629	90.76 ppm (d, 197.2 Hz)	Rh^{III}NO$^-$	[40]

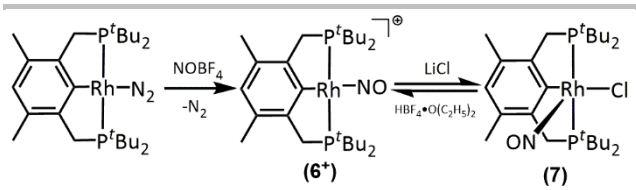

Scheme 2. Obtention of **(6⁺)** and **(7)**.

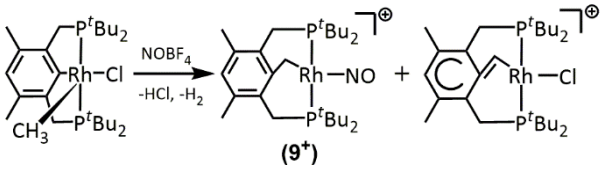

Scheme 3. Obtention of **(9⁺)**.

Although most of the work published by our group has been focused on these complexes,[28,41,42] in recent years we have also explored reactivity of a complex with an asymmetric PCN pincer scaffold.[40] In this case, obtention of the tetradentate species proved to be challenging, since the route analogous to that shown in Scheme 2 yielded pentacoordinate Rh(PCN)(NO)(Cl) **(20)** due to residual chloride in solution. Three separate nitrosylation pathways were tested: using a dinitrogen precursor with $NOBF_4$, using a hydride precursor and isoamyl nitrite, and using a hydride precursor and Diazald® (N-methyl-N-nitroso-p-toluenesulfonamide). This last alternative was ultimately chosen for having the best conversion and most efficient work-up. Since all three pathways yielded Rh(PCN)(NO)(Cl) **(20),** an extra chloride abstraction step had to be introduced to obtain the tetracoordinate species $[Rh(PCN)(NO)]^+$ **(19⁺)**, as shown in Scheme 4.

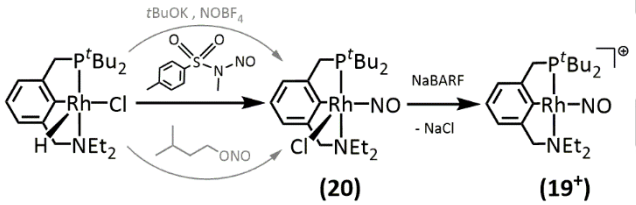

Scheme 4. Three pathways for obtention of **(19⁺)**.

Both **(6⁺)** and **(19⁺)** present a rich redox chemistry which is further revised in the following section. In particular, their reduced analogues **(6•)** and **(19•)** displayed interesting reactivities of their own. These were obtained by the one-electron reduction of these first stable species with cobaltocene in benzene solution under argon.

2.2. Electrochemical studies

As it has already been discussed, the NO ligand can adopt either NO^+, $NO^•$ or NO^- configurations. The ability to perform these rearrangements turns it into a potential electron reservoir. Therefore, the effect of the pincer ligand on the electron transfer behavior of nitrosyl complexes is of particular interest, although it is relatively unexplored.

An interesting study on the matter for rhodium complexes with similar pincer ligands is summarized in Table 3. These have been based on studies performed for complexes **(6⁺)** and **(7)** (PCP), **(9⁺)** ($PC^{CH2}P$), and **(19⁺)** and **(20)** (PCN). As can be seen, all of the linear tetracoordinate complexes undergo a one-electron reduction at a relatively accessible potential yielding a $\{RhNO\}^9$ species. As can be seen from $E_{1/2}$ values, changing of the pincer arms did not have a significant effect in this reduction, whereas exchanging phenyl by benzyl coordination does make the reduction less favorable, due to increased donation to the metallic center. Notably, the analogous complex Rh(PCP)(CO)[43] does not present a reduction within the THF solvent window, which proves that the redox reactivity in these species is indeed a direct consequence of nitric oxide's redox versatility. For PCP and $PC^{CH2}P$ a second irreversible reduction, which has not been included in Table 3, was observed at around -2.5 V. This was not observed for PCN due to the narrower solvent window. Irreversibility is believed to be caused by loss of either the NO or the pincer ligand.

Table 3. $E_{1/2}$ vs ferrocene obtained by cyclic voltammetry experiments for three related pincer nitrosyl complexes, expressed in volts.

	L=PCP	L=$PC^{CH2}P$	L=PCN
$[Rh(L)(NO)]^+ + e^- \rightarrow [Rh(L)(NO)]^•$	-1.16 (r)	-1.41 (r)	-1.19 (i)
$Rh(L)(NO)Cl \rightarrow [Rh(L)(NO)(Cl)]^{+•} + e^-$	0.65 (i)	0.65 (i)	0.68 (r)
$[Rh(L)(NO)]^+ \rightarrow [Rh(L)(NO)]^{2+} + e^-$	--	--	1.02 (qr)

(r)= reversible, (i)= irreversible, (qr)= quasi-reversible.

The oxidations available for these species also deserve some observations. Most notable in this aspect is the fact that only the PCN complex presented an oxidation of the tetracoordinate linear NO species. This is consistent with the more electron donating character of the amine group in PCN compared to the phosphine, which favors higher oxidation states. Such an effect has already been reported for a similar asymmetric pincer complex, in a work carried out by Wendt's group for complexes lacking a nitrosyl ligand.[44] A more subtle consequence of this electronic effect is the fact that for oxidation of the pentacoordinate bent NO species the oxidation is reversible for PCN (and irreversible for PCP and $PC^{CH2}P$), which also hints of a slight stabilization of higher oxidation states. It is also remarkable that this irreversible oxidation presents the same value of $E_{1/2}$ for both PCP and $PC^{CH2}P$. In this case, the $Rh^{III}NO^-$ species has less electron back-donation to the metallic center and so the difference in donation between the phenyl and benzyl ligands has virtually no effect on the reduction potential.

As for the case of PNP pincer complex **(8^{2+})**, electrolytic reduction of this complex resulted only in an irreversible reduction within the solvent window, coupled with oxidations that were later demonstrated to belong to a $[Rh(PNP)(CH_3CN)]^+$ species. A $[Rh(PNP)(NO)(Cl)]^+$ analogue was prepared by reaction of **(8^{2+})** with LiCl, but its cyclic voltammetry showed a similar behavior.

Therefore, the one-electron reduction for PNP $\{RhNO\}^8$ complexes results in loss of the nitric oxide ligand, as was confirmed by separate FTIR spectroelectrochemistry experiments where the ν(NO) band was seen to disappear during electrolytic reduction, and so no further studies on them were performed.[45]

Given the efficiency of using ν(NO) FTIR signal as a probe for presence and configuration of nitric oxide, relevant redox processes reported in Table 3 have been explored by FTIR spectroelectrochemistry (SEC). Some are summarized in Figure 4.

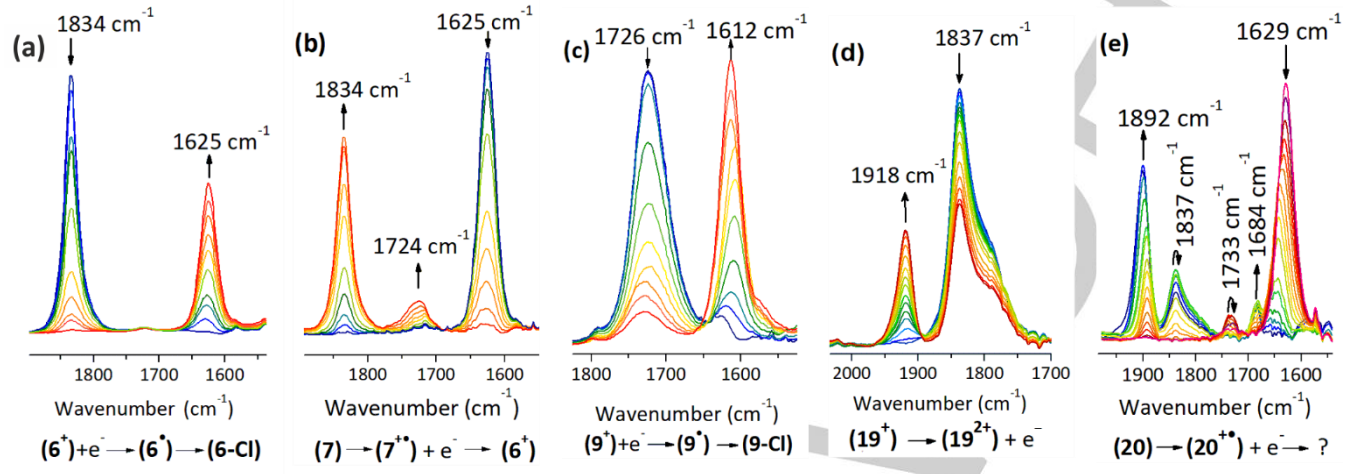

Figure 4. FTIR-SEC experiments performed for: **(a)** Reduction of **(6⁺), (b)** Oxidation of **(7)**, **(c)** Reduction of **(9⁺)**, **(d)** Oxidation of **(19⁺)**, **(e)** Oxidation of **(20).**

Figures 4a and 4c present the electrolytic reduction of **(6⁺)** and **(9⁺)** in CH_2Cl_2, respectively. As can be observed, reduction resulted in loss of the linear ν(NO) signals and emergence of bent ν(NO) signals at around 1620 cm^{-1}. Moreover, although cyclic voltammetry experiments showed a reversible reduction, no linear ν(NO) signal was recovered by reverting the potential. This proves there is a different reactivity occurring in these experiments: most likely intermediate unstable 17-electron **(6•)** and **(9•)** species, which can be reverted by one-electron oxidation back to their precursors, are in this case reacting further with the solvent and abstracting a chloride atom from it. This suspected reaction was confirmed by conducting the chemical reduction of both complexes in CH_2Cl_2 and identifying their products as the pentacoordinate chlorinated species. Isolation of reduced {RhNO}[9] was of interest given the scarce bibliography on this sort of complexes. As was made apparent from electrochemical experiments in CH_2Cl_2, these studies had to be carried in non-chlorinated solvents to ensure a relative stability for the expected product. Further studies on this reactivity are discussed in a separate section of this review.

Figures 4b and 4e present the electrolytic oxidation of Rh(L)(NO)(Cl) complexes **(7)** and **(20)**. There are a few similarities between both processes. Both present linear ν(NO) signals corresponding to their respective $[Rh(L)(NO)]^+$ species and intermediate ν(NO) signals at around 1730 cm^{-1} which are attributed to $[Rh(L)(NO)(Cl)]^{+\bullet}$ unstable **(7⁺•)** and **(20⁺•)** species. One explanation for these observed signals could be that whereas one-electron oxidation occurs, the unstable radical species reacts losing $Cl^•$ and yielding the linear species and Cl_2. Interestingly, there are also some differences between both of these experiments. Firstly, while for oxidation of **(7)**, the signal of the linear product **(6⁺)** consistently grows throughout the experiment, for the oxidation of **(20)**, signal of **(19⁺)** is seen to grow at first but to diminish later on. This is a result of the ability of **(19⁺)** to be further oxidized. Effectively, at higher potentials oxidation of **(19⁺)** is evidenced by appearance of a 1918 cm^{-1} overlapped with that of the main product at 1892 cm^{-1} (*vide infra*). More evident is the fact that oxidation of **(20)** presents even more signals that have no correlation whatsoever with those observed for **(7)**, evidencing a more complex or even an altogether separate oxidation pathway. Remarkably, when chemical oxidation of **(20)** was tested, only these signals (1684 cm^{-1} and 1892 cm^{-1}) were observed, and the paramagnetic character of these complexes was confirmed by their lack of signals in ^{31}P-NMR. No further studies on this peculiar oxidation have been carried out yet.

Figure 4d presents the electrolytic oxidation of the four-coordinate complex **(19⁺)**, which as has been mentioned is of interest since no other pincer made this process possible. As can be seen, **(19⁺)** partially oxidizes without loss of the nitric oxide ligand yielding a **(19^{2+})** complex. Although the intensity for the reverse reduction is scarce, as seen in cyclic voltammetry experiments, partial recovery of the initial complex was achieved by reverting of the potential. Since an $Rh^{I}NO^+$ configuration is expected for this complex, it would be reasonable to expect this oxidation to be centered in the Rh atom. No further studies could be carried out since attempts at chemical oxidation only resulted in decomposition of **(19⁺)**.

Pecak and coworkers have also exploited the nitrosyl ligand as a probe for electrolytic oxidation. In their case, a Co(PCP)(NO)(Cl) **(17)** complex, {CoNO}[8] in Feltham notation, was observed to oxidize reversibly in $E_{1/2}$=0,11 V vs ferrocene. FTIR-SEC showed conversion from the bent 1654 cm^{-1} ν(NO) signal of **(17)** to a new ν(NO) signal of 1771 cm^{-1} for the {CoNO}[7] product. However, the MNO configuration for this species could not be conclusively assigned. Whereas the ν(NO) shift suggested linearization of the nitrosyl ligand, and therefore a NO-centered oxidation, DFT calculations did not reflect this experimental observation neither in the CoNO calculated angle (which only changed from 143.5° to 148.2°) nor in the spin density, which was localized in the metallic center.[39]

2.3. Pincer nitrosyls in catalysis and bond activation

One of the ultimate aims of research into pincer nitrosyl complexes is the design of efficient catalysts for a number of organic reactions. Since these particular types of complexes are still relatively unexplored, there are little reports of them being used as catalysts. Choualeb and coworkers' rhenium hydride complex **(2)** has been proven to work as a catalyst for transfer hydrogenation of ketones, but decomposition of the complex under their experimental conditions limited the reaction.[36] Fogler et al. reported dehydrogenative coupling of alcohols to esters to be catalyzed by ruthenium complex **(12)**.[37] Complex **(16)** was shown to be catallytically active for the coupling of primary alcohols to amines, whereas complex **(15)** catalyzed the hydrosilylation of ketones.[30,31] Pecak and coworkers' have also studied the use of a cobalt hydride complex derived from **(18$^+$)** as a catalyst for the hydroboration of alkenes, and have used DFT calculations to elucidate the mechanism involved. Interestingly, they found nitrosyl to play an important par, since strong bending of the CoNO angle and its reversion were found to be involved, thus revealing the ligand to act as a reservoir of electrons (Scheme 5).[32]

Activation of carbon-halogen bonds leading to formation of new carbon-carbon bonds is also of interest for organic synthesis. Instability of complex **(6$^\bullet$)** in CH_2Cl_2 hinted of an interesting reactivity of the sort for our {RhNO}^{9} complexes with organic halides which has been further explored.[40,41] However, a more controlled -and thus, more tunable- reactivity would result from coordination of the organic moiety to the metallic center. This has not been observed for either complex, although reduction of the steric bulk by changing from PCP to PCN could have been expected to favor it. The effect of further reducing steric hindrance in the pincer is yet to be studied.

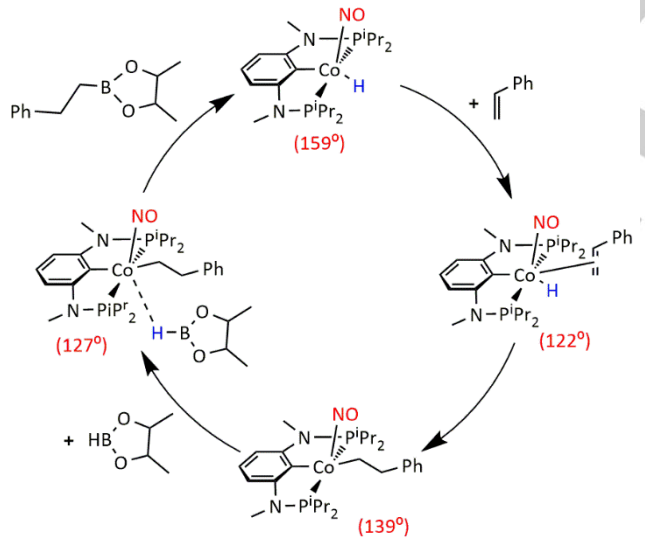

Scheme 5. Catalytic cycle for the hydroboration of alkenes as proposed by Kirchner and coworkers.[32] DFT-calculated Co-N-O angles are indicated in red.

Most notable was reaction with 2-fluoroiodobenzene substrate, which bears the advantage of allowing ^{19}F-NMR monitoring. Both for **(6$^\bullet$)** or **(19$^\bullet$)** the reaction observed was that depicted by Scheme 6. Presence of [Rh(L)(NO)(I)] was detected by ^{31}P-NMR and confirmed by separate preparation and characterization of this new complex. Formation of 2-fluorobiphenyl was detected by ^{19}F-NMR and confirmed by GC-MS. This implies that abstraction of I$^\bullet$ from the substrate is effected by the radical complex, yielding a radical substrate byproduct which in turn activates the benzene solvent. Similar reactivity was found for other tested substrates.

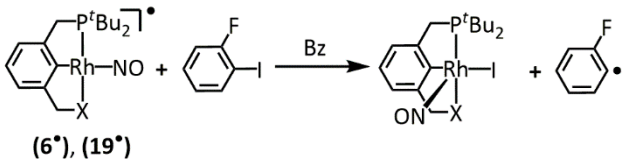

Scheme 6. Activation of 2-fluoroiodobenzene by **(6$^\bullet$)** (X=P^{t}Bu$_2$) and **(19$^\bullet$)** (X=NEt$_2$).

2.4. NO disproportionation

Interconversion between NO$^\bullet$ and NO_x, N_2O, etc., is relevant in environmental chemistry given that these species are known air-pollutants.[46] Disproportionation of NO$^\bullet$ is one of the possible interconversion routes, particularly significant due to the fact that NO$^\bullet$ rarely undergoes this reaction unless assisted by a catalyst. This reaction is also catalyzed in biological systems by nitrite reductases,[47] so its biological significance is not to be underrated either.

Verat and coworkers have thoroughly studied disproportionation of NO$^\bullet$ by reaction with a Rh(I)PNP complex.[26] Interestingly, their precursor is actually a Rh(III) complex prone to reductive elimination and thus a source of masked Rh(I). Reaction with several Rh/NO$^\bullet$ ratios has been studied (Scheme 7), where the main product Rh(PNP)(NO)(NO$_2$) **(5)** could be identified in higher NO$^\bullet$ ratios. Presence of Rh(PNP)(NO)$^\bullet$ in low Rh:NO ratios suggest it to be an intermediate. A separate experiment using pure Rh(PNP)(N$_2$) and adding NO$^\bullet$ was carried out, which showed complete conversion to **(5)**, thus explaining the absence of this product in higher Rh:NO$^\bullet$ ratios.

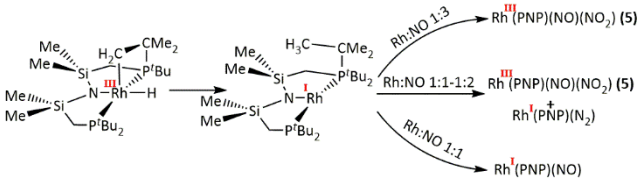

Scheme 7. Experiments with varying ratios of Rh:NO$^\bullet$ carried out by Verat et al.[26]

The complete disproportionation reaction as proposed by the authors is presented in Scheme 8. Further research on the mechanism did not shed much light into it. An unknown intermediate consistent with Rh(PNP)(X)(Y) - due to its C_S symmetry - was observed in experiments with low NO$^\bullet$ ratio. Its identity was inquired by exploring geometry optimization by DFT calculations of several possible intermediates, out of which the structure was defined as Rh(PNP)(NO)(ONO).

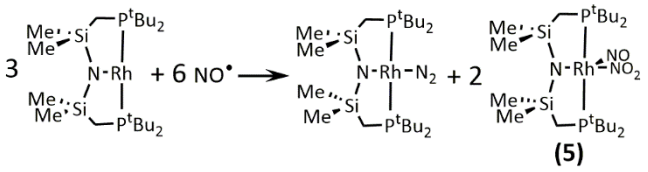

Scheme 8. Reaction equation of Rh(PNP) and nitric oxide.

The authors propose that since the first intermediate Rh(PNP)(NO)• is a 17 electron species, coordination of a second NO• radical is most likely to occur, thus yielding an unseen intermediate Rh(PNP)(N_2O_2), which could be either a dinitrosyl species or a hyponitrite one, depending on the free NO• attack site. Two alternative pathways are proposed. Firstly, reaction of the undefined Rh(PNP)(N_2O_2) with Rh(PNP)(NO)• to yield Rh(PNP)(NO_2) -which in turn yields the final product by binding another NO• molecule- and Rh(PNP)(N_2O) which subsequently decomposes to Rh(PNP(N_2) by oxygen transfer to either the nitrosyl or the dinitrosyl species. The second alternative consists of an oxygen transfer from Rh(PNP)(N_2O_2) to free NO• resulting in free NO_2• which can then bind the nitrosyl intermediate. The authors believe this last mechanism to be more appropriate given that the steric bulk introduced by pincer PNP might interfere with O-atom transfer between pincer-complexes.

We have also studied the NO• disproportionation reaction mediated by a rhodium pincer complex.[42] This reactant consists of a radical {RhNO}^{9} species (coincidentally the same configuration as the Rh(PNP)(NO)• intermediate observed by Verat et. al.). The reaction both of [Rh(PCP)(NO)]• **(6•)** and of Rh(PCP)(N_2) were followed by FTIR (Scheme 9). The main difference comparing to the previous work is that the reaction products differ from those observed by Verat et al.: whereas a Rh(PCP)(NO)(NO_2) was formed, no dinitrogen complex is observed. The reduced NO product was instead free N_2O, as detected by FTIR gas spectroscopy, which is actually the most frequently reported product for transition metal complex-assisted NO disproportionation. The authors have acknowledged this particularity by suggesting intermediate Rh(PNP)(N_2O) as part of a proposed mechanism.

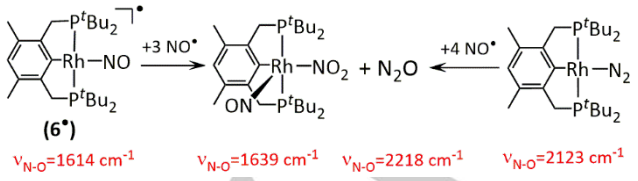

Scheme 9. Reactions of [Rh(PCP)(NO)]• and of Rh(PCP)(N_2) with NO.

Notably, N_2O could already be detected when adding only one equivalent of NO. This, together with observation of an isosbestic point between the FTIR signals of [Rh(PCP)(NO)]• and Rh(PCP)(NO)(NO_2), suggests a fast reaction with short-lived intermediates. Effectively, no intermediates were detected in the FTIR experiments. As has already been discussed in the previous work,[26] some sort of Rh(PCP)"N_2O_2" formulation would be expected as an intermediate, either as a dinitrosyl or as a hyponitrite complex. In order to elucidate the mechanism involved, both DFT calculations and mixed-labeling experiments were undertaken.

Reaction of [Rh(PCP)(^{15}NO)]• with ^{14}NO yielded both Rh(PCP)(^{14}NO)(NO_2) and Rh(PCP)(^{15}NO)(NO_2), along with signals for all possible combinations of labeling for nitrous oxide: $^{14}N_2O$, $^{14}N^{15}NO$, $^{15}N^{14}NO$ and $^{15}N_2O$. This reveals that there is indeed formation of a dinitrosyl species, which is in turn in equilibrium with both its mononitrosyl species (Scheme 10). Dinitrosyl species containing pincer ligands are relatively rare, but reports of both chemically equivalent and nonequivalent NO structures can be found.[34,48] However, the existence of a hyponitrite species cannot be discarded.

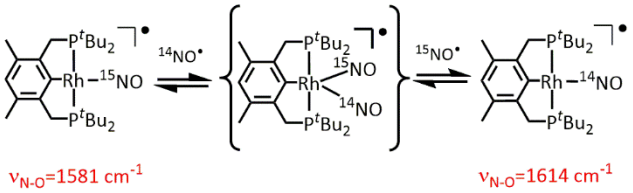

Scheme 10. Equilibrium between the mononitrosyl species and the dinitrosyl intermediate.

DFT geometry optimizations led to comparable energies for possible dinitrosyl and hyponitrite intermediates. Either of these intermediates should react with a third molecule of nitric oxide releasing a N_2O molecule and resulting in a [Rh(PCP)(NO_2)]• intermediate complex, which in turn binds another nitric oxide molecule to yield the final product. Isolation of the new paramagnetic intermediate [Rh(PCP)(NO_2)]• was attempted by reaction of [Rh(PCP)(NO)]• with O_2, but Rh(PCP)(O_2) and Rh(PCP)(NO)(NO_2) were obtained instead of the desired product (*vide infra*).

A few observations on the work carried out by Watson et al. are pertinent with regard to NO• disproportionation.[48] In this work, reactivity of a 14-electron Ru(PNP)Cl (note that the pincer ligand is much similar to that used by Verat et. al.) with NO• was studied (Scheme 11). Although the authors were unable to isolate and identify the main product, an interesting structure was elucidated by XRD from crystals obtained only under excess NO•: the ion pair [Ru(PNP)($NO)_2$][Ru(NO)(OH)Cl_2($NO_2)_2$] **(21^+)**. The authors propose the overall unusual reactivity to derive from instability of the suspected primary product Ru(PNP)(NO)Cl• - a radical species - which favors further reaction with NO•, the only radical quencher present in the reaction mixture. An expected byproduct of this reaction would be free nitrous oxide, although its presence was not verified, along with nitrite, which was found to bind Ru in the counteranion. The authors discarded secondary reactions with N_2O to be responsible for the convoluted reactivity observed by running a control experiment of Ru(PNP)Cl with N_2O and confirming no reaction to take place.

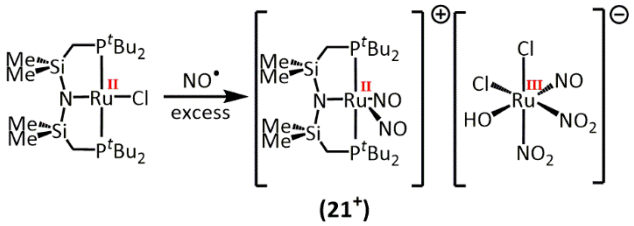

Scheme 11. Reaction of Ru(PNP)(Cl) with excess NO yielding **(21^+)**.

Remarkably, in the dinitrosyl cation nitrosyl ligands present an NO^+ and an NO^- configuration (*vide infra*), and **(21$^+$)** can therefore be considered a Ru(II) complex, just as the Ru(PNP)Cl precursor, thus having mediated the NO• disproportionation without a global redox change. However, the counteranion has not only undergone oxidation to Ru(III) but has also lost the pincer ligand. It cannot be completely discarded that NO• disproportionation has not taken place mediated by this complex, since the presence of dinitrosyl is highly suggesting, but a mechanism could not be proposed.

2.5. Dinitrosyl complexes

Pincer dinitrosyl species are rarely reported. However, they are often invoked as intermediates in a number of reactions, especially in NO• disproportionations, as we have already discussed (Scheme 10). Dinitrosyl iron complexes have been proposed to function as biological reservoirs and carriers of NO, oftentimes being prone to NO• - releasing decomposition pathways. Currently, reports of this type of species are mainly focused on structural studies and do not thoroughly explore their reactivity.

An early and rather peculiar case was reported by Watson et al.,[48] which has already been presented in Scheme 11. The $[Ru(PNP)(NO)_2]^+$ complex reported is particularly interesting since it features two chemically inequivalent molecules of nitric oxide. One of them, located *trans* to the amine of the pincer ligand, presented a linear NO^+ configuration with a Rh-N-O angle of 178.9°. The other one, positioned in the apical site of the square-based pyramid, presented a bent NO^- configuration with a Rh-N-O angle of 129.0°.

Another relevant report was made by Suzuki et al. with a rather unusual bulky SNS thioamide pincer ligand.[34] The first challenge faced in the work was the synthesis of a monochelate complex rather than the most easily obtained *bis*-chelate species. The authors solved this by employing a bulky pincer ligand. Exposure of $Fe(SNS)(THF)_2$ to a nitric oxide atmosphere resulted in formation of the dinitrosyl compound $Fe(SNS)(NO)_2$ **(22)** as is presented in Scheme 12. Differently from the previous case, this complex features two chemically equivalent nitric oxide molecules. XRD-elucidated structure consists of a trigonal bipyramidal structure with the pincer moiety located in the trigonal plane and the two NO molecules with Fe-N-O angles of 168.9° and 168.0°. N-O bond lengths are reported to be 1.154(4) and 1.166(3) Å, longer than NO^+, shorter than NO^- and very similar to neutral NO• radical. The authors suggest the two unpaired electrons in the metallic Fe(II) center and the two NO• radicals to be coupled antiferromagnetically. Interestingly, although most $\{Fe(NO)_2\}^8$ structures tend to be susceptible to decomposition into $\{FeNO\}^7$ and free NO•, this is not seen for the reported complex.

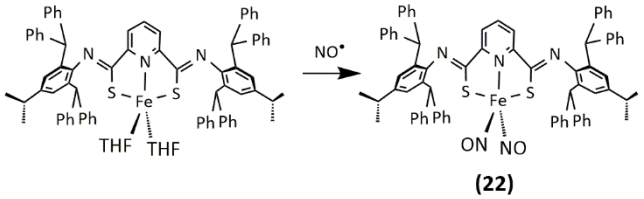

(22)

Scheme 12. Obtention of $Fe(SNS)(NO)_2$ **(22)**.

2.6. Other reactivities

The sensitivity of the characteristic ν(NO) FTIR signal to the electronic influence of the ambiance means that the nitrosyl ligand can be used as a probe for changes in the coordination sphere. A brief but elegant example was presented by Pecak et al., who worked with cobalt complexes of three identical PCP pincer ligands with different linker groups: CH_2, NCH_2 and O.[39] The consequently decreasing donor strength for the pincer ligand, which in turn decreases back donation from the metal center to the nitrosyl ligand, was reflected by the increasing ν(NO) signal shift, as can be seen in Figure 5.

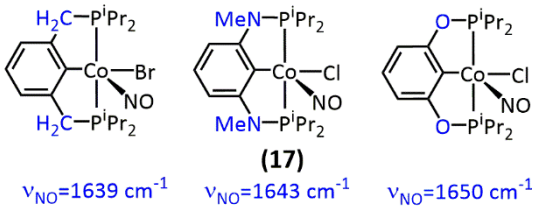

Figure 5. Cobalt pincer complexes with different linkers and their ν(NO) signal.

Another example is the analysis of solvent influence on the nitrosyl group carried out for complex **(6$^+$)**.[28] Three parameters for the solvents were taken into account for this study: the Gutmann donor number (DN), the Gutmann acceptor number (AN) and the Z-value. The first two numbers rank organic solvents by their ability to either donate or accept electron density, respectively, whereas the Z-value is a measure of solvent polarity. As can be seen in the results presented in Figure 6, there was a clear tendency towards higher frequency ν(NO) signals with decrease on the DN or increase on the AN. The effect of the Z-value also showed a slightly less marked tendency towards decrease of the ν(NO) signal with increased polarity. These tendencies are proof that solvents can indirectly interact with the nitric oxide ligand through the metallic center: good donors enhance the electron density of the metallic center and so increase back donation from rhodium to NO, decreasing ν(NO). Good acceptors, on the other hand, drain electron density from the rhodium and so impede efficient back donation towards NO, increasing ν(NO).

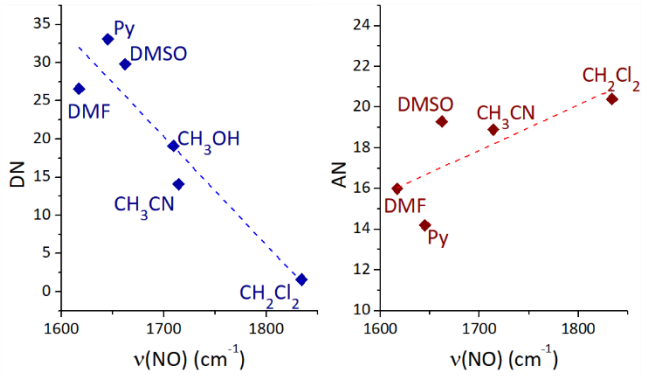

Figure 6. FTIR NO frequencies for complex **(6$^+$)** in several solvents versus: **(left)** their DN numbers; **(right)** their AN numbers.

Interestingly, the large shifts in v(NO) caused by some highly donor solvents indicate that the effect of back donation is actually causing the NO to switch from a linear configuration to a bent one. This was confirmed separately by analysis of the ^{31}P-NMR signals. Therefore, for these cases, it might be more appropriate to consider the solvent as a fifth ligand, as is depicted in Scheme 13. Although DN and AN are defined for second-sphere solvent effects, coordinating solvents still show a good correlation with non-coordinating ones. Notably, all of these equilibria could be displaced back to a linear configuration by subjecting the solution to vacuum and redisolving in a suitable solvent. An extreme case was seen in the case of **(19$^+$)**, where exposure of the complex to CH_3CN resulted in formation of the pentacoordinate species $[Rh(PCN)(NO)(NCCH_3)]^+$ that could not be reversed even under high vacuum for several hours.[40] This relative stability when compared to PCP of coordinated CH_3CN introduced by the PCN ligand could be attributed to the reduced steric hindrance of the latter. However, it could be also related to the more electron-donating character of the PCN ligand, favoring Rh(III) complexes.

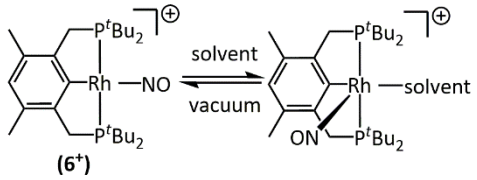

Scheme 13. Reaction of **(6$^+$)** with highly electron-donating solvents.

Another such extreme case was seen only for derivatives of PCN complex **(19$^+$)**.[40] As has already been mentioned, this complex was obtained via Rh(PCN)(NO)(Cl) **(20)** following chloride abstraction with NaBArF (BArF$^-$=tetrakis[3,5-bis(trifluoromethyl)phenyl]borate). When this was attempted with salts of other weakly-coordinating anions (WCAs), namely $TlBF_4$, $TlPF_6$ and silver triflate (AgOTf), **(19$^+$)** could not be isolated, and instead coordination of the WCAs was observed. In the case of AgOTf, reaction with one equivalent yielded only Rh(PCN)(NO)(OTf). However, in the case of BF_4^- and PF_6^- an equilibrium between $[Rh(PCN)(NO)^+][X^-]$ **(A)** and [Rh(PCN)(NO)(X)] **(B)** (X= BF_4^-;PF_6^-) was established. In both cases, addition of extra tetrabutylammonium hexafluorophosphate resulted in an increased v(NO) **(A)** signal. This is evidence that structure **(B)** in the equilibrium is formed not by any X^- anion in solution but by the X^- counteranion inside of the ionic pair structure, that is to say, the counteranion in the most immediate proximity (Scheme 14). Hence, the addition of more counteranion X^- results not in further coordination of it, since it cannot access the ionic pair structure, but instead increases the ionic pair stability by increasing the ionic strength of the solution. All of these experiments were carried out in dichloromethane, so it would be reasonably expected for a more polar solvent to also have an effect in this equilibrium, although this was not studied. Although WCAs have been proved not to be completely inert in several reports,[49–52] this case bears the advantage that the nitric oxide ligand makes WCA coordination easily detectable by FTIR.

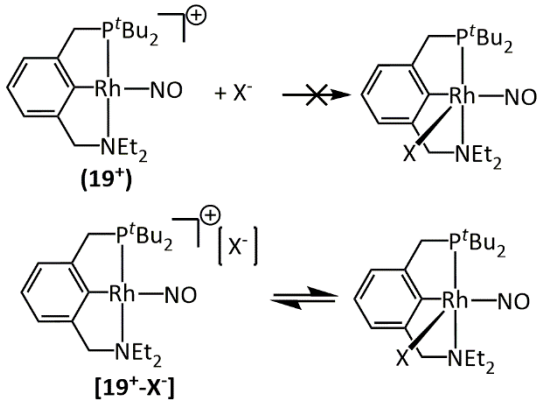

Scheme 14. Equilibrium established between $[Rh(PCN)(NO)^+][X^-]$ **(A)** and [Rh(PCN)(NO)(X)] **(B)**.

A similar linear to bent equilibrium was reported both for PCP and PCN in the case of reaction with carbon monoxide.[28,40] Upon addition of gaseous CO to a linear NO solution of either **(6$^+$)** or **(19$^+$)**, the presence of the new $[Rh(L)(NO)(CO)]^+$ was detected by appearance of two FTIR bands (one split band corresponding to v(CO) at around 2080 cm^{-1} and one corresponding to v(NO) at around 1700 cm^{-1}). However full conversion did not take place and the linear v(NO) did not disappear even under treatment with excess CO. Interestingly, the equilibrium could be fully displaced by removing CO under vacuum.

Stabilization of small molecules is also of importance. Oxygen adducts have been reported for other pincer complexes,[43] their significance lying in the chemical and structural insight they can give both in oxygenation processes -for complexes able to activate molecular oxygen - and in oxygen transport - for complexes able to reversibly coordinate to oxygen. Milstein and coworkers explored the formation of oxygen adducts using **(11$^+$)** as a precursor complex, and studied the mechanistics of oxygen transfer to assess their possible reactivity in catalytic oxidation cycles.[53]On the other hand, both {RhNO}^{9} complexes **(6$^\bullet$)** and **(19$^\bullet$)** have been found to be short-lived and particularly air sensitive. Reaction of **(6$^\bullet$)** with O_2 was tested in an attempt to isolate a NO$^\bullet$ disproportion intermediate, but instead it was found to result in coordination of oxygen to the metallic center, as is shown in Scheme 15.[42] However for the case of the PCN ligand, whereas reaction of **(19$^\bullet$)** with air does also yield $[Rh(PCN)(NO)(NO_2)]$, coordination of the oxygen molecule was not observed.[40] Reaction with excess O_2 resulted in decomposition of **(19$^\bullet$)** into several products as evidenced by ^{31}P-NMR (unpublished data).

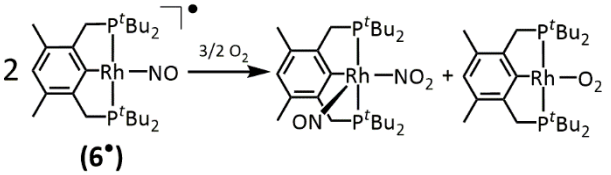

Scheme 15. Reaction of **(6$^\bullet$)** with O_2.

Non-innocence of the pincer ligand, although frequent in the literature, has seldom been reported for pincer nitrosyl complexes.

One of the few cases is the dearomatization of rhodium complex **(11$^+$)** to form **(12)**,[37] which has also been observed for **(11$^+$)**'s oxygen adduct (Scheme 16).[53] The interest in this type of reactivity lies in the possible implications for catalytic cycles involving pincer complexes, where aromatization-dearomatization could enable the activation of chemical bonds. MNO angles and FTIR ν(NO) values for **(11$^+$)** and **(12)** are omitted in Scheme 16 as they have already been presented in Table 1. These last values for the dearomatization process are, however, unexpected, since reducing of the total charge could be expected to reduce ν(NO) rather than increase it. Similarly, the completely reversible formation of a protonated arene featuring an agostic interaction between the metal iron center of a structural analogue of **(16)** and the transient C-H bond has also been reported.[22]

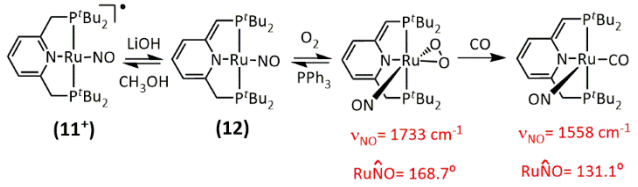

Scheme 16. Dearomatized pincer nitrosyl products reported by Milstein and coworkers and their interconversion.

3.Nitrosyl and nitroxyl porphyrin complexes

As mentioned in the Introduction, a great part of the studies involving nitroxyl stabilization and characterization have been carried out using porphyrins as ligand platforms, due to their special significance as heme enzyme bioinorganic models. In particular, this has been one of the main subjects of our research group. In the following sections, our own progress in this field will be discussed, along with the most relevant pioneering antecedents.

3.1.{MNO}$^{6/7}$ porphyrin complexes

Depending on the different electronic properties of each transition metal, nitrosyl complexes may be best described as M-NO$^+$, M-NO$^\bullet$ or M-NO$^-$/M-HNO species. Some iron-based platforms have allowed for the redox interconversion between all three states,[54–58] but this is not the case for all metals. For example, almost all porphyrin complexes with manganese centers have a linear {MnNO}^{6} electronic structure, although isomerism to bent species has also been observed.[59] These complexes are probably best described as Mn(I)-NO$^+$ species, which show greater stability compared to iron {FeNO}^{6} analogues. This makes manganese porphyrin nitrosyls good models for the more elusive ferric heme nitrosyls.[60,61] Further reduction of these complexes takes place on the porphyrin ring, yielding unstable compounds which release NO$^\bullet$, and so {MnNO}$^{7/8}$ are neither easily accessible nor useful for studying the reactivity of reduced MNO species.[62] However, there is early evidence for a {MnNO}^{7} complex formed at 77K via γ irradiation,[63] and reactive intermediates of this nature may be present in NO$^{\bullet-}$ disproportionation and electrocatalytic nitrite reduction mediated by Mn porphyrins.[64,65]

{MNO}$^{6/7}$ porphyrin complexes can be prepared by different methods, such as bubbling NO$^\bullet$ gas into a solution of a porphyrin bearing a metal center which readily binds NO$^\bullet$, like Fe(II) or Ru(II); or either via reductive nitrosylation or nitroxyl trapping reactions on a more oxidized center, namely Fe(III), or Mn(III).[66–69] Both NO$^\bullet$ porphyrin species have been thoroughly and meticulously studied by other pioneering groups, and complete literature analyzing their stability along with kinetic and mechanistic aspects of their reactivity is available.[25,47,70] Although these efforts have mainly been focused on iron coordinated systems, Ru, Co, Os, Mn, Cr and Mo nitrosyl porphyrin complexes have also been widely studied and reviewed in detail.[67,71–80]

In the following section, focus will be put mainly in revisiting porphyrin nitroxyl (HNO and NO$^-$) complexes, mainly of iron, which represent an important research topic in our laboratory over the last decade.

3.2 {MNO}^{8} porphyrin complexes

Iron

Iron nitroxyl complexes can be prepared, from their {FeNO}$^{6\text{-}7}$ precursors, via chemical/electrochemical reduction of a Fe(II)-NO$^\bullet$ derivative, or through direct hydride attack on a Fe(II)-NO$^+$ species. Although the first {FeNO}^{8} moiety was found in a dinitrosylporphyrin complex,[81] reports on mononitrosyl species of this kind come from Kadish and coworkers, who made substantial advance in the field of iron nitroxyl porphyrin complexes, working with the TPP (*meso*-tetraphenylporphyrinate) and OEP (*β*-octaethylporphyrinate) platforms. The Fe(II)-NO$^-$ adducts **(23$^-$)** and **(24$^-$)** were obtained from their nitrosyl precursors in dichloromethane by electrochemical reduction (Figure 7).[82,83]

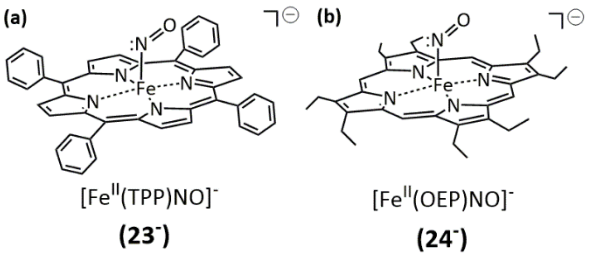

Figure 7. The first examples of iron nitroxyl porphyrin complexes, Fe(TPP)NO$^-$ **(23$^-$)** and Fe(OEP)NO$^-$ **(24$^-$)**.

Years later, Ryan's group managed to further stabilize these same NO$^-$ products in THF solution also via chemical and electrochemical means, enabling their characterization by FT-IR spectroscopy. [84,85] Evidence for the Fe-HNO derivatives was also subsequently gathered, via electrochemical studies of the nitrosyls in the presence of weak acids;[86] the [Fe(OEP)(HNO)] adduct resulted stable for hours, as long as a phenols were present as proton sources.[87] The HNO complex was proposed to be stabilized by hydrogen bonds with phenol molecules. Abucayon and coworkers obtained the hexacoordinated, imidazole bound variant [Fe(OEP)(HNO)(5-MeIm)] from the ferric nitrosyl using a hydride attack strategy in chloroform, allowing its characterization via ^{1}H NMR giving a 11% yield at -20°C.[88] This hydride reduction approach had already been successfully carried out by Lee and Richter-Addo in the same pioneering group, which resulted in the preparation, in 77% yield, of the first porphyrin

HNO complex **(25)** using the [Ru(TTP)(5-MeIm)] platform (TTP: *meso*-tetratolylporphyrinate) in methanol (Scheme 17).[89] This adduct could be properly characterized via FT-IR and ^{1}H NMR, and this kind of reactivity later allowed carbon-nitrogen and nitrogen-nitrogen bond formation by alkyl attack on Fe(II)-NO^{+} and Ru(II)-NO^{+} porphyrin complexes.[90] The presence of a sixth axial ligand is key for effective HNO formation, since hydride can coordinate directly to the metal center instead if there is an available position.[91]

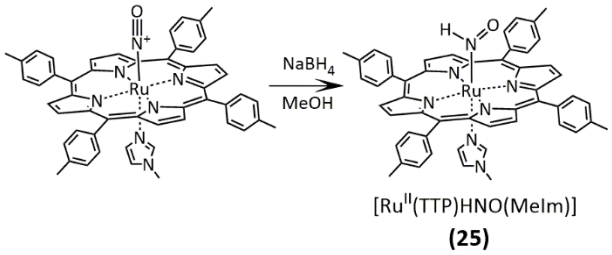

Scheme 17. Formation of the first porphyrin HNO complex via hydride attack on coordinated NO^{+}.

In 2010, the first {FeNO}^{8} complex could be isolated by Pellegrino and coworkers in our research group, taking advantage of a very electron withdrawing perhalogenated porphyrin, TFPPBr$_8$ (β-octabromo-*meso*-tetrakis-(pentafluorophenyl)porphyrinate), which provided extra stability towards oxidation.[92] [Fe(TFPPBr$_8$)(NO^{-})]$^{-}$ **(26^{-})** (Figure 8) was obtained by chemical reduction of the corresponding {FeNO}^{7} adduct using cobaltocene, and proved to be indefinitely stable in deoxygenated CH_2Cl_2 solution. The protonated HNO complex could not be experimentally observed, since acid addition instantaneously yielded the starting [Fe(TFPPBr$_8$)(NO$^{\bullet}$)] species. Nevertheless, the perhalogenated platform allowed for ^{15}N NMR characterization of an iron nitroxyl anion complex for the first time, with a resonance signal at +790 ppm vs $CH_3{}^{15}NO_2$, proof of its diamagnetic nature and the {FeNO}^{8}configuration. Further FT-IR and UV-Vis spectroscopic characterization, along with DFT theoretical calculations, interestingly suggested the assignment of the electronic structure of **(26^{-})** as an intermediate between Fe(II)-NO^{-} and Fe(I)-NO$^{\bullet}$ states, rather than establishing it as a predominantly ferrous nitroxyl complex as stated for other related non-heme, low spin complexes.[93]

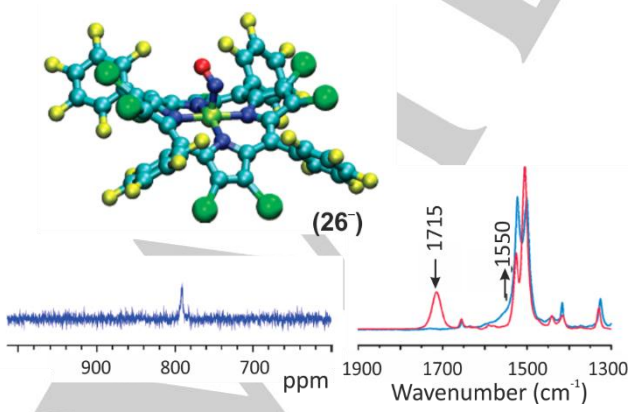

Figure 8. DFT structure of **(26^{-})** (top); ^{15}N NMR signal of Fe(TFPPBr$_8$)(NO^{-}) at 790 ppm (bottom left); IR spectra of the nitrosyl (red) and nitroxyl (blue) derivatives (bottom right).

The observed spontaneous reoxidation upon acid addition to yield the nitrosyl Fe(II)-NO$^{\bullet}$ adduct gave rise to the possible hypothesis of a bimolecular decomposition of Fe(P)HNO complexes, (Eq. 1) with formation of hydrogen gas. This was later supported by results obtained with a sterically hindered porphyrin by Lehnert and coworkers.[94]

$$2Fe^{II}(P)HNO \rightarrow 2Fe^{II}(P)NO^{\cdot} + H_2 \quad (1)$$

This particularly electron poor substituted porphyrin even allowed for the investigation of a second reduction of the nitrosyl complex, which displayed a reversible wave in performed cyclic voltammetry experiments (Figure 9).[95] The product, [Fe(TFPPBr$_8$)(NO)]$^{2-}$ could be characterized by UV-Vis and FT-IR in solution. The N-O stretch frequency, which was expected to lower due to the increased electron density, was observed to shift from 1550 to 1590 cm^{-1} instead. DFT calculations predicted such a behavior for intermediate and high spin complexes (with S = 3/2 and 5/2), but not for low spin states (S = ½). Moreover, the calculated higher bond angle for the Fe-N-O moiety in the optimized structures also suggested a porphyrin ring-based reduction and delocalization, giving a structure best described as a [{FeNO}^{7}(TFPPBr$_8$)$^{4-}$]$^{2-}$ species.

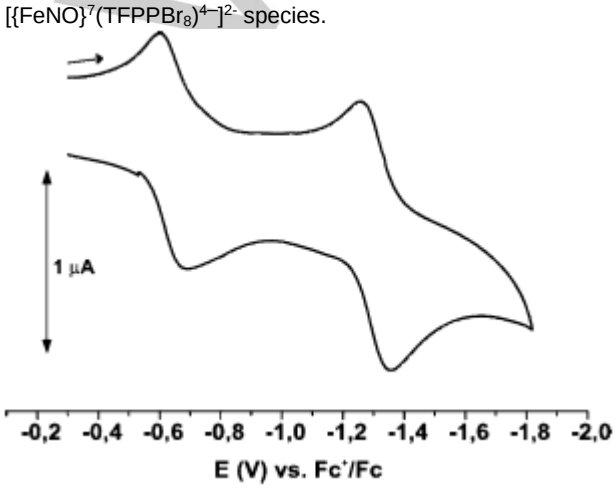

Figure 9. Cyclic voltammetry of Fe(TFPPBr$_8$)NO showing its two reversible reduction processes. Reproduced from reference [92].

In the last five years the crystal structures of **(26^{-})** as well as that of **(24^{-})** could be resolved, shedding more light in the field of hemenitroxyl compounds.[4,96] Of particular interest is the experimental evidence of the expected increased bending of the Fe-N-O adducts, displaying angles of 122° and 127° respectively, compared to their nitrosyl precursors at 148.5° and 143°.

The use of electron poor porphyrinic platforms was further exploited by Goodrich and coworkers, who observed similar results for different complexes in dichloromethane and THF solution. Remarkably, a *bis picket fence* porphyrin with bulky substituents (3,5-Me-BAFP^{2-} 3,5-methylbis(aryloxy)-fence porphyrin dianion) provided them with a robust scaffold for obtaining the first ferrous heme model HNO complex **(27)**, which displays outstanding stability as it gives back the corresponding nitrosyl precursor only after several hours (Figure 10).[94] These results supported the hypothesis of the bimolecular decomposition (Eq. 1), since the sterically hindered coordination site prevents two HNO moieties from approaching each other and reacting to produce molecular hydrogen.

Table 4. Selected porphyrin nitrosyl complexes and their relevant spectroscopic parameters.

{M-NO}[8] Porphyrin/heme Complex	ν_{NO} (cm^{-1}) ($^{14}N/^{15}N$)	**H**NO ^{1}H-NMR (ppm)	Ref.
Fe(TPP)(NO^+)(NO^-)	1690[a]	-	[81]
Fe(OEP)(NO^-)	1440/1425[b]	-	[85]
Fe(OEP)(5-MeIm)(HNO)	1383/1360[c]	13.99 ($CDCl_3$)	[88]
Ru(TTP)(5-MeIm)(HNO)	1380/1348[d]	13.64 ($CDCl_3$)	[89]
Fe(TFPPBr$_8$)(NO^-)	1550[e]		[92]
Fe(3.5-Me-BAFP)(NO^-)	1466		[94]
Fe(To-F_2PP)(NO^-)	1473		[94]
Fe(To-$(NO_2)_2$-p-tBuPP)(NO^-)	1482		[94]
Fe(T*per*-F_5TPP)(NO^-)	~ 1500		[94]
Mb-HNO	1385[f]	14.8 (20% D_2O buffer)	[97,98]
IgHb-HNO (leghemoglobin)		15.0 (phosphate buffer)	[99]
cHb-HNO (hemoglobin I)		15.53 (phosphate buffer)	[99]
hHb-HNO (human hemoglobin)		14.63, 14.80 (phosphate buffer)	[99]
Co(TPP)(NO)	1689[d]		[100]
Co(OEP)(NO)	1660		[101]
Co(T(*p*-OCH_3)PP)(NO)	1680[h]		[102]
Co(T(*p*-NO_2)PP)(NO)	1694[h]		[102]
Co(TMPyP)($NO)^{4+}$	1722[g]		[103]
Co(T(X)PP)(NO) X = *p*-CH_3, *p*-OCF_3, *p*-CF_3, *p*-CN, *m*-CH_3, *m*-OCH_3	1681-1695[h]		[104]
Co(TPPBr$_4$$NO_2$)(NO)	1692[c]		[105]
Co(CTPPMe)(NO) (*N* confused)	1620[d]		[106]

a: Nujol; b: THF solution; c: $CHCl_3$ solution; d: KBr solid; e: solid film/CH_2Cl_2 solution; f: from XANES/XAFS measurements; g: Data from resonance Raman; h: CH_2Cl_2 solution.

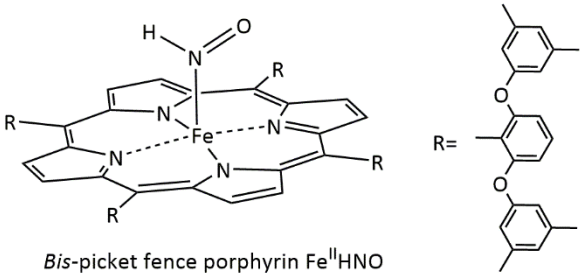

Bis-picket fence porphyrin $Fe^{II}HNO$

(27)

Figure 10. Fe-HNO complex of a bis-picket fence porphyrin.

The first well characterized HNO heme complex was in fact that of myoglobin in aqueous media, reported by Lin and Farmer, for which ^{15}N and ^1H NMR spectra were successfully obtained.[97] This adduct was stable for weeks, and allowed further characterization by Raman spectroscopy and X-ray absorption,[98] as well as setting a precedent for the preparation of new HNO complexes of other globins through different strategies, making the special stability of these protein adducts evident.[99] Despite the many reports of evidence for different {MNO}^{8} reported in organic media that emerged in the years following this breakthrough, which were already revisited, no characterization of a water soluble nitroxyl porphyrinic complex occurred until for almost another two decades.

In 2019, the ferrous nitrosyl complex based on the widely used, water-soluble anionic porphyrinic platform TPPS (*meso*-tetraphenylsulphonate porphyrin dianion), could be isolated in our group by Mazzeo and coworkers. The convenient manipulation of Na_4[Fe(TPPS)(NO$^\bullet$)] as an isolated solid allowed us to further study its redox behaviour and some properties of its nitroxyl derivatives.[107] An earlier study which explored the flash photolysis reduction of the Fe(II)-NO$^\bullet$ complex by a benzophenone ketyl radical, which yielded a transient species attributable to a nitroxyl complex,[108] inspired us to use this porphyrinate as a suitable platform for the study of the elusive {FeNO}^{8} form.

After optimizing the experimental conditions to ensure maximum oxygen exclusion, the {Fe**H**NO}^{8} derivative **(28^{4-})** could be obtained in pH 6 phosphate buffer, via chemical reduction with recrystallized sodium dithionite,[109] as monitored by UV-Vis spectrophotometry. The characteristic porphyrin Soret band shifted its position from 414 to 418 nm (Figure 11), accompanied with a more evident 40% increase in molar absorptivity; similar changes were observed in early studies involving flash photolysis reductions of [Fe(TPPS)(NO$^\bullet$)]$^{4-}$ generated in situ. Analogous experiments at pH 12 resulted in a different, more subtle spectra transformation, in which the more noticeable changes were in the Q-band zone (Figure 11), surprisingly similar to the observed spectral changes for the reduction of {FeNO}^{7} porphyrynate complexes in organic media.[94] Our tentative assignments of the reduction product at pH 6 as [Fe(TPPS)(HNO)]$^{4-}$ **(28^{4-})**, and the product at pH 12 as [Fe(TPPS)(NO^-)]$^{5-}$ **(29^{5-})** were confirmed as both products interconverted upon base and acid addition respectively. It is important to note that, while the deprotonated nitroxyl complex appeared to be only sensitive to possible oxygen filtrations, the HNO adduct **(28^{4-})** quickly reverted to the nitrosyl adduct, and so base addition had to proceed immediately after Fe-HNO formation.

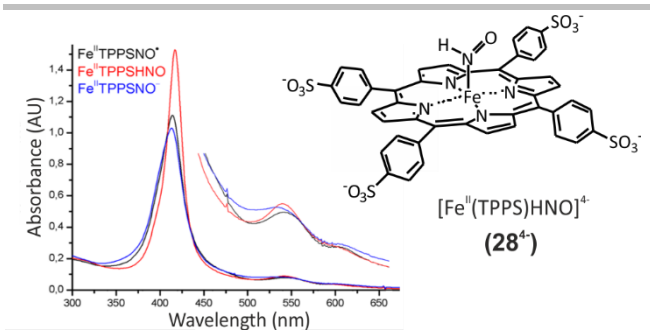

Figure 11. UV-Vis spectra for the nitrosyl and nitroxyl derivatives of [Fe(TPPS)]$^{4-}$ (left) and structure of **(28^{4-})** (right).

The obtention of both protonated and deprotonated nitroxyl adducts allowed for a systematic spectroscopic and electrochemical characterization as a function of pH. UV-Vis experiments showed the Fe-HNO species to dominate up to pH 9, while the Fe-NO^{-} adduct was the only reduction product from pH 10 and above. Concordantly, the pH dependence of the reduction potential satisfyingly fitted to the behavior predicted by the Nernst equation for a p*K*a of 9.7 (Figure 12), with E_{RED} values of -0.665 vs. Ag/AgCl for [Fe(TPPS)(NO$^{\bullet}$)]$^{4-}$,H^{+}/**(28^{4-})** at pH 6 (in concordance to electrochemical pioneering studies of the *in situ* generated nitrosyl by Meyer),[110] and E_{RED} = -0.885 V for [Fe(TPPS)(NO$^{\bullet}$)]$^{4-}$/**(29^{5-})** at pH = 11.3. The estimated p*K*a value for **(28^{4-})** is about two units lower than the reported value of 11.4 for free HNO,[111] in agreement with the stabilization of the NO^{-} moiety due to coordination. This result is of special relevance, being the first of its kind reported for a heme porphyrin complex, and allowing a biomimetic model useful for exploring the reactivity of heme enzymes of the nitrogen cycle.

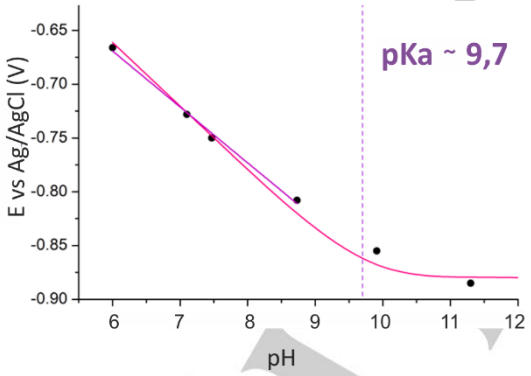

Figure 12. Experimental measurements of the reduction potential of [Fe(TPPS)(NO$^{\bullet}$)]$^{4-}$ as a function of pH. Nernst equation for pKa = 9.7 is plotted in pink. The experimental slope of the purple plot is -52 mV/pH, in fair agreement with Nernst's prediction of -59 mV/pH.

The spontaneous reoxidation reaction of **(28^{4-})** was kinetically studied under different experimental conditions resulting in a first-order (and not second order, as proposed by Eq.1) decomposition with k = (0,017 ± 0,003) s^{-1}, which did not change significantly with pH, and resulted ≈ 3 times smaller in D_2O. When the radical TEMPO was added to the cuvette once **(28^{4-})** was formed, instant and complete formation of the {FeNO}^{7} nitrosyl was observed, evidencing the relatively weak nature of the H-N bond in the HNO moiety, for which an upper limit value of 70 kcal/mol can be established.[112] These results suggested a decomposition pathway involving the homolytic cleavage of such bond as the rate-limiting step. DFT calculations with [Fe(TPP)(HNO)] supported this hypothesis, evidencing the migration of the hydrogen atom from the HNO moiety to the most proximate *meso* carbon of the porphyrin ring to form a *phlorin radical* intermediate, when scans increasing the H-N bond distance of the HNO moiety were performed (Figure 13). The *phlorin radical* structure resulted only 2.4 kcal mol^{-1} higher in energy than the initial complex, while the calculated activation energy resulted in 19.4 kcal mol^{-1}, in agreement with experimental measurements of k_{OBS} as a function of temperature, which yielded an experimental activation energy of approximately 13 kcal/mol. Intramolecular PCETs of this kind have been recently reported for other porphyrins, where the bent *phlorin* intermediate was theoretically proposed and detected.[113,114] With this in mind, a decomposition mechanism consisting of a rate-limiting step involving H-NO homolytic cleavage and phlorin formation followed by fast porphyrin rearomatization and H atom loss was proposed. Further spectroscopic and reactivity characterization of these complexes is the subject of ongoing work.

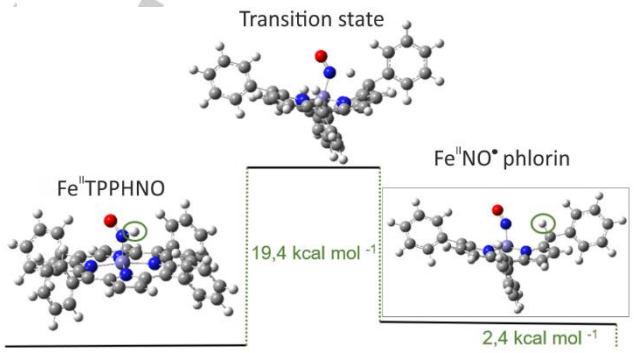

Figure 13. DFT structures for the Fe(TPP)(HNO) model, calculated transition state and phlorin intermediate for the proposed decomposition.

All in all, the fundamental factors affecting the stability of {Fe-**H**NO}^{8} complexes are not completely clear. Although in organic media the bimolecular reaction (Eq. 1) might be the principal decomposition pathway, as supported by the enhanced stability provided by hindered porphyrins,[94] more evidence should be gathered to make ends meet, especially regarding the formation of H_2 gas as a byproduct. In aqueous media, however, there seem to be additional and diverse reasons influencing the stability of protonated HNO adducts. For instance, the heme protein adducts studied by Farmer and coworkers are particularly stable because of strong hydrogen bond formation between the nitroxyl moiety and distal amino acid residues. More specifically, evidence from NOESY experiments along with computational simulations support hydrogen bonding interaction of a Histidine residue and the oxygen atom in the HNO species, among others. This kind of interactions favour a specific configuration of the nitroxyl adduct, possibly providing additional stability due to electronic as well as steric effects.[97,115] The remarkable stability reported for the non-heme {FeNO}^{8} nitroxyl complex [Fe(CN)$_5$(HNO)]$^{3-}$ allowed for the determination of the first apparent p*K*a value for bound HNO, and yet they bear no bulky ligands that might provide special

protection.[54] The only other water-soluble porphyrin HNO derivative, $[Fe(TPPS)(HNO)]^{4-}$, although not as long-lived as the former, presents enhanced stability compared to structurally similar complexes in organic media (and, in addition, appears to decompose by an unimolecular pathway, not proposed before for nonaqueous media). Very interestingly, in a recent report from 2019, Rahman and Ryan provided evidence for the formation of a hydrogen bonded complex $Fe(OEP)(NO^{-})\cdots$H-O-Ph in addition of the protonated [Fe(OEP)(HNO)] adduct in the presence of substituted phenols acting as weak acids.[116] The existent equilibrium (shown in Figure 14) between both species is strongly temperature dependent, and illustrates the importance of considering hydrogen bonding interactions when analyzing the stability of Fe-HNO adducts.

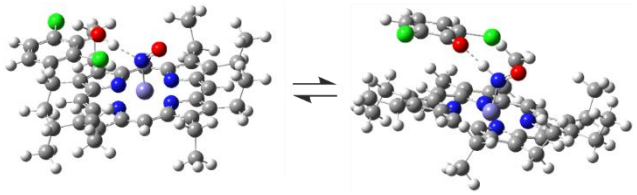

Figure 14. Proton transfer-hydrogen bonding equilibrium for $Fe(OEP)(NO^{-})\cdots$H-O-Ph and $Fe(OEP)(HNO)\cdots$—O-Ph. Reproduced from reference [116]. Copyright 2019, with permission from American Chemical Society.

All these observations put together make us consider whether the interaction of the nitroxyl complexes with more polar solvent water molecules or buffer species themselves might provide additional stability. Moreover, the newly proposed decomposition mechanism for Fe-HNO complexes involving a *phlorin* intermediate provides a new interpretation for the remarkable stabilities of the water soluble HNO complexes $[Fe(CN)_5(HNO)]^{3-}$ [54] and $[Ru(Me_3[9]aneN_3)(bpy)(HNO)]^{1+}$,[117] which do not have this route available. In the case of the *bis-picket-fence* adduct **(27)**, this could be prevented due to the high steric hindrance of the *meso* carbon.[94] In this context, research focusing on the stability and reactivity of nitroxyl heme complexes in aqueous and organic media remains an interesting challenge for bioinorganic chemists.

Cobalt

The first reported nitroxyl complex was in fact not an iron complex, but [Co(TPP)(NO)], in 1973.[100] Evidence in this work and many others, show that most readily prepared Co-NO porphyrin complexes fall in the $\{CoNO\}^8$ category, displaying complementary reactivity to that explained above for Mn-NO porphyrin complexes.[118] These adducts present Co-N-O angles of ~ 120° and diamagnetism, and so are best described as Co(III)-NO^{-} entities.[104,105] They are also five-coordinated due to the strong trans-effect caused by the nitroxyl ligand, although some six-coordinate adducts were detected at low temperatures. $\{CoNO\}^8$ complexes can be prepared by reaction of Co(II) porphyrins, either in solution or in solid state, with gaseous NO via a reductive nitrosylation mechanism,[119,120] or either by reaction with nitrosonium ion (NO^{+}) followed by chemical reduction of the Co(II)-NO^{+} adduct using cobaltocene.[104]

Several spectroscopic and electrochemical studies on related complexes came to the conclusion that the $\{CoNO\}^{6/7}$ derivatives are not easily accessible, since oxidation of the nitroxyl complexes occurs on the porphyrin ligands to give a π radical cation[101]. Even if the first reduction is reversible in the voltammetric timescale, the second process eventually yields Co(III) species and free NO.[104,105,118,121] Interestingly, results from spectroelectrochemical studies in organic media showed changes in the ν_{NO} frequency during the first and second oxidation that were consistent with formation of π cations on the porphyrin system still bearing the NO moiety.[102,121] On the other hand, reduction experiments ended in NO labilization after the first reductive process.[121] Using a perbromated, nitro-substituted porphyrin, Kadish and coworkers could relatively stabilize the one and two-electron reduction products, which conserved the NO moiety on a short timescale, suggesting a reduction process based on the electron withdrawing macrocycle.[105] Interestingly, this porphyrin exhibited a saddled conformation; later studies have shown that tetrapyrrole distortion can trigger different changes in Co-NO binding mode[122] and reactivity, as shown by N_2O production from nitrite catalyzed by an isolated $\{CoNO\}^9$ complex based on the N-confused porphyrin system **(30^{-})**, in which the nitrogen atom is now at the β position of one of the pyrrole groups, and coordination occurs via a carbon atom (Figure 15).[106]

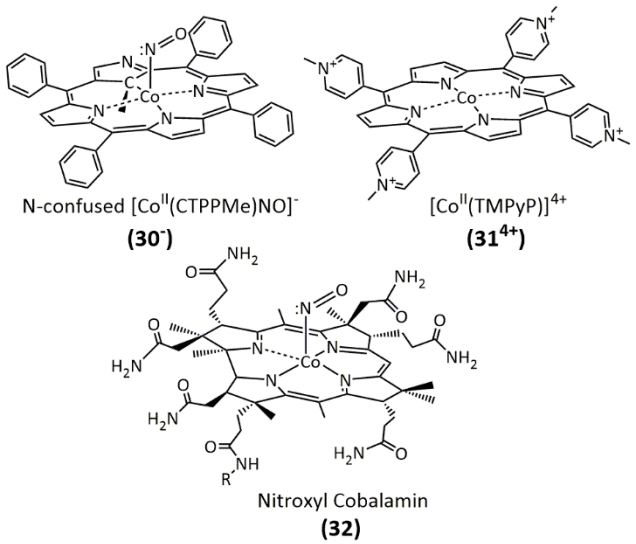

Figure 15. Structure of N-confused porphyrin nitroxyl cobalt complex $Co(CTPPMe)(NO^{-})$ (*top left*), $Co(TMPyP)^{4+}$ (*top right*) and simplified nitroxyl cobalamin (*bottom*).

In aqueous media, the reductive nitrosylation of Co(II) porphyrins to give Co(III)-NO^{-} adducts was performed with many derivatives,[120] and in particular $[Co(TMPyP)]^{4+}$ **(31^{4+})** can act as a catalyst for nitrite reduction to ammonia, implying the possible formation of Co(III)-HNO or Co(II)-HNO intermediates, even if such complexes have not been directly observed.[103]

Although not strictly a porphyrin but a structurally related corrole, cobalamine, also known as Vitamin B12, is a biologically relevant compound bearing Co(III) atoms in a corrin structure. Cobalamin was found to react with nitric oxide in both its natural and its reduced Co(II) form, to give a $\{CoNO\}^8$ complex, **(32)**, characterized again as a diamagnetic Co(III)-NO^{-} complex by ^{15}N NMR experiments.[123–125]

In contrast to iron, HNO cobalt porphyrin adducts are not observed, since protonation takes place on the macrocycle rather

than on the nitroxyl ligand.[126] However, {CoNO}^{8} complexes can show HNO donor reactivity in the presence of protons,[126] an ability also shared by a non-porphyrin {CoNO}^{9} complex with promising HNO-release reactivity in aqueous media.[127] This complex is very well characterized, and interpreted as a Co(II)-NO^- entity, which releases HNO upon protonation. Many non-porphyrin {CoNO}^{n} complexes have been prepared and reviewed, and computational studies of porphyrinic derivatives have been performed.[128,129] Some of them are proposed as reactive intermediates in the catalytic reduction of nitrite to ammonium.[130]

Summary and Outlook

The pincer nitrosyl organometallic complexes chemistry is an incipient but growing field which has considerably advanced in the last decade. The synthesis and structural elucidation of several new pincer nitrosyl complexes, assisted by detailed electrochemical studies, led to the discovery of remarkable transformations. Among the most important results we can mention the selective activation and functionalization of C-X (X= Cl, Br, I) bonds; mediation of NO disproportionation by different rhodium complexes; some sparse reports of catalytic activity for specific organic reactions, which are yet to be more consistently studied but constitute a promising subject of study, where the assistance of the NO as an electron reservoir has already begun to be observed. In particular, the activation of C-X bonds by {RhNO}^{9} complexes with PCP and PCN pincer ligands implies that halide abstraction and single-electron transfer chemistry is not limited to first-row transition metals, thanks to the ability of NO to act as electronic "accumulator".

Moreover, the reversible CO addition to four-coordinate {RhNO}^{8} complexes **(6$^+$)** and **(19$^+$)** could be of potential application to sensors in solid or crystalline state, whereas reversible coordination of solvents to complex **(6$^+$)** and of WCAs to **(19$^+$)** are also remarkable results. This reversible coordination is again a manifestation of nitric oxide's redox activity, since it takes place through interconversion between linear NO^+ and bent NO^-.

All in all, NO is a powerful electron reservoir that in combination with pincer complexes can offer interesting possibilities for future applications in catalysis and bond activation. A lot of chemistry is waiting to be studied on this topic, and the combination of the NO redox activity with the cooperativity of PNP pincer ligands as proton shuttles will certainly give place to interesting chemistry in proton-coupled electron transfer processes, such as the hydrogen evolution reaction.[131]

On the other hand, nitroxyl, is becoming increasingly popular due to its biological effects, which only partially overlap those of NO$^\bullet$, showing functions of its own. It has also been shown to be easily produced from by mild, biologically relevant reducing agents.[132] Hemoproteins are one of the main biological targets of these small molecules and heme {FeNO}$^{6\text{-}8}$ adducts have become a particularly interesting object of study from a bioinorganic point of view.

The remarkable increase in the number of reports on {FeNO}^{8} complexes during the last decade has contributed to the spectroscopic characterization of this initially elusive species, although further studies are still required to obtain detailed information at the mechanistic level. More than a decade ago, a particularly stable {FeNO}^{8} complex **(26$^-$)**, could be isolated and characterized by UV-Vis, FT-IR and ^{15}N-NMR in our laboratory using a perhalogenated, electron-deficient porphyrin in organic medium. More recently, chemical reduction of a water-soluble heme {FeNO}^{7} precursor at different pH values resulted in the formation of the first water-soluble heme nitroxyl complexes, {FeNO}^{8} **(29^{5-})** and {Fe**H**NO}^{8} **(28^{4-}).** UV-Vis characterization of these complexes, added to the electrochemical information obtained from cyclic voltammetry experiments of the {FeNO}^{7} complex allowed us to estimate the pKa of the {Fe**H**NO}^{8} species at around 9.7. More importantly, we could establish a mechanism for the first-order decay of the {Fe**H**NO}^{8} complex, that involves ligand cooperativity of the porphyrinate, forming a *phlorin* intermediate in which the hydrogen atom from the HNO moiety has migrated to the most proximate *meso* carbon of the porphyrin ring. Further studies to get more insight in this novel heme {Fe**H**NO}^{8} decomposition mechanism are needed.

The ever-expanding literature on nitric oxide coordination compounds reflects the rich chemistry offered by the NO-metal interaction, with many fundamental aspects still to be learned and lots of new applications continuously appearing. To take a case in point, the first transition metal nitrosyl, $[Fe(NO)(H_2O)_5]^{2+}$, the iconic "Brown-Ring" chromophore, was discovered by Joseph Priestley more than two hundred years ago,[133] but even today there are reports on new aspects of its electronic structure, with its DRX structure elucidated just in 2019.[134] Surely, with the aid of promising scaffolds such as pincer ligands and porphyrinates, a lot of new fascinating metal nitrosyl chemistry is yet to be discovered.

Acknowledgements

The research reported in this publication was supported by the Ministerio de Ciencia y Tecnología e Innovación Productiva (PICT-2015-3854, PICT-2017-1930 and PICT 2017-1877) and the Universidad de Buenos Aires (UBACYT) project # 20020170100595BA.

All authors are CONICET members. C.M.G., and A.M. are doctoral students, while C.G., J.P. and F.D. are faculty researchers.

Keywords: Complexes; Nitrosyl; Nitroxyl; Pincer; Porphyrin

References

[1] J. H. Enemark, R. D. Feltham, *Coordination Chemistry Reviews* **1974**, *13*, 339–406.
[2] W. R. Scheidt, Y. J. Lee, K. Hatano, *J. Am. Chem. Soc.* **1984**, *106*, 3191–3198.
[3] M. K. Ellison, W. R. Scheidt, *J. Am. Chem. Soc.* **1997**, *119*, 7404–7405.
[4] B. Hu, J. Li, *Angew. Chem. Int. Ed.* **2015**, *127*, 10725–10728.
[5] C. J. Moulton, B. L. Shaw, *J. Chem. Soc., Dalton Trans.* **1976**, 1020–1024.
[6] N. A. Al-Salem, H. D. Empsall, R. Markham, B. L. Shaw, B. Weeks, *J. Chem. Soc., Dalton Trans.* **1979**, 1972–1982.
[7] J. Errington, W. S. McDonald, B. L. Shaw, *J. Chem. Soc., Dalton Trans.* **1980**, 2312.
[8] C. Crocker, H. D. Empsall, R. J. Errington, E. M. Hyde, W. S. McDonald, R. Markham, M. C. Norton, B. L. Shaw, B. Weeks, *J. Chem. Soc., Dalton Trans.* **1982**, 1217–1224.
[9] M. Albrecht, G. van Koten, *Angew. Chem. Int. Ed.* **2001**, *40*, 3750–3781.

[10] G. van Koten, K. Kirchner, M.-E. Moret, Eds. , *Metal-Ligand Co-Operativity: Catalysis and the Pincer-Metal Platform*, Springer International Publishing, Cham, **2021**.
[11] G. Van Koten, R. A. Gossage, *The Privileged Pincer-Metal Platform: Coordination Chemistry & Applications*, Springer, **2015**.
[12] D. Morales-Morales, *Pincer Compounds: Chemistry and Applications*, Elsevier, **2018**.
[13] E. Poverenov, D. Milstein, in *Organometallic Pincer Chemistry* (Eds.: G. van Koten, D. Milstein), Springer Berlin Heidelberg, Berlin, Heidelberg, **2013**, pp. 21–47.
[14] E. Poverenov, M. Gandelman, L. J. W. Shimon, H. Rozenberg, Y. Ben-David, D. Milstein, *Chem. - Eur. J.* **2004**, *10*, 4673–4684.
[15] D. Vuzman, E. Poverenov, L. J. W. Shimon, Y. Diskin-Posner, D. Milstein, *Organometallics* **2008**, *27*, 2627–2634.
[16] E. Poverenov, M. Gandelman, L. J. W. Shimon, H. Rozenberg, Y. Ben-David, D. Milstein, *Organometallics* **2005**, *24*, 1082–1090.
[17] E. Poverenov, G. Leitus, L. J. W. Shimon, D. Milstein, *Organometallics* **2005**, *24*, 5937–5944.
[18] A. Fleckhaus, A. H. Mousa, N. S. Lawal, N. K. Kazemifar, O. F. Wendt, *Organometallics* **2015**, *34*, 1627–1634.
[19] R. Lindner, B. van den Bosch, M. Lutz, J. N. H. Reek, J. I. van der Vlugt, *Organometallics* **2011**, *30*, 499–510.
[20] A. J. Ruddy, S. J. Mitton, R. McDonald, L. Turculet, *Chem. Commun.* **2012**, *48*, 1159–1161.
[21] S. Hosokawa, J. Ito, H. Nishiyama, *Organometallics* **2012**, *31*, 8283–8290.
[22] D. Himmelbauer, M. Mastalir, B. Stöger, L. F. Veiros, M. Pignitter, V. Somoza, K. Kirchner, *Inorg. Chem.* **2018**, *57*, 7925–7931.
[23] C. Gunanathan, D. Milstein, *Acc. Chem. Res.* **2011**, *44*, 588–602.
[24] C. M. Frech, L. J. W. Shimon, D. Milstein, *Angew. Chem. Int. Ed.* **2005**, *44*, 1709–1711.
[25] G. B. Richter-Addo, R. A. Wheeler, C. A. Hixson, L. Chen, M. A. Khan, M. K. Ellison, C. E. Schulz, W. R. Scheidt, *J. Am. Chem. Soc.* **2001**, *123*, 6314–6326.
[26] A. Y. Verat, M. Pink, H. Fan, B. C. Fullmer, J. Telser, K. G. Caulton, *Eur. J. Inorg. Chem.* **2008**, *2008*, 4704–4709.
[27] B. C. Fullmer, M. Pink, H. Fan, X. Yang, M.-H. Baik, K. G. Caulton, *Inorg. Chem.* **2008**, *47*, 3888–3892.
[28] C. Gaviglio, Y. Ben-David, L. J. Shimon, F. Doctorovich, D. Milstein, *Organometallics* **2009**, *28*, 1917–1926.
[29] J. Mason, L. F. Larkworthy, E. A. Moore, *Chem. Rev.* **2002**, *102*, 913–934.
[30] D. Himmelbauer, B. Stöger, L. F. Veiros, M. Pignitter, K. Kirchner, *Organometallics* **2019**, *38*, 4669–4678.
[31] J. Pecak, B. Stöger, M. Mastalir, L. F. Veiros, L. P. Ferreira, M. Pignitter, W. Linert, K. Kirchner, *Inorg. Chem.* **2019**, *58*, 4641–4646.
[32] J. Pecak, S. Fleissner, L. F. Veiros, E. Pittenauer, B. Stöger, K. Kirchner, *Organometallics* **2021**, *40*, 278–285.
[33] M. Feller, E. Ben-Ari, T. Gupta, L. J. W. Shimon, G. Leitus, Y. Diskin-Posner, L. Weiner, D. Milstein, *Inorg. Chem.* **2007**, *46*, 10479–10490.
[34] T. Suzuki, J. Matsumoto, Y. Kajita, T. Inomata, T. Ozawa, H. Masuda, *Dalton Trans.* **2014**, *44*, 1017–1022.
[35] V. M. Krishnan, H. D. Arman, Z. J. Tonzetich, *Dalton Trans.* **2018**, *47*, 1435–1441.
[36] A. Choualeb, A. J. Lough, D. G. Gusev, *Organometallics* **2007**, *26*, 3509–3515.
[37] E. Fogler, M. A. Iron, J. Zhang, Y. Ben-David, Y. Diskin−Posner, G. Leitus, L. J. W. Shimon, D. Milstein, *Inorg. Chem.* **2013**, *52*, 11469–11479.
[38] A. Walstrom, M. Pink, H. Fan, J. Tomaszewski, K. G. Caulton, *Inorg. Chem.* **2007**, *46*, 7704–7706.
[39] J. Pecak, W. Eder, B. Stöger, S. Realista, P. N. Martinho, M. J. Calhorda, W. Linert, K. Kirchner, *Organometallics* **2020**, *39*, 2594–2601.
[40] C. M. Gallego, C. Gaviglio, Y. Ben-David, D. Milstein, F. Doctorovich, J. Pellegrino, *Dalton Trans.* **2020**, *49*, 7093–7108.
[41] J. Pellegrino, C. Gaviglio, D. Milstein, F. Doctorovich, *Organometallics* **2013**, *32*, 6555–6564.
[42] C. Gaviglio, J. Pellegrino, D. Milstein, F. Doctorovich, *Dalton Trans.* **2017**, *46*, 16878–16884.
[43] C. M. Frech, L. J. W. Shimon, D. Milstein, *Helv. Chim. Acta* **2006**, *89*, 1730–1739.
[44] A. H. Mousa, J. Bendix, O. F. Wendt, *Organometallics* **2018**, *37*, 2581–2593.
[45] J. Pellegrino, Complejos de Metales de Transición Con El Ligando Rédox Activo NO: Estructura Electrónica, Interconversión, y Reactividad, PhD thesis, University of Buenos Aires, **2012**.
[46] W. C. Trogler, *J. Chem. Educ.* **1995**, *72*, 973.
[47] L. E. Goodrich, F. Paulat, V. K. K. Praneeth, N. Lehnert, *Inorg. Chem.* **2010**, *49*, 6293–6316.
[48] L. A. Watson, M. Pink, K. G. Caulton, *J. Mol. Catal. A: Chem.* **2004**, *224*, 51–59.
[49] W. Beck, K. Suenkel, *Chem. Rev.* **1988**, *88*, 1405–1421.
[50] M. Gandelman, L. Konstantinovski, H. Rozenberg, D. Milstein, *Chem. - Eur. J.* **2003**, *9*, 2595–2602.
[51] T. M. Douglas, E. Molinos, S. K. Brayshaw, A. S. Weller, *Organometallics* **2007**, *26*, 463–465.
[52] P. W. Blosser, J. C. Gallucci, A. Wojcicki, *Inorg. Chem.* **1992**, *31*, 2376–2384.
[53] E. Fogler, I. Efremenko, M. Gargir, G. Leitus, Y. Diskin-Posner, Y. Ben-David, J. M. L. Martin, D. Milstein, *Inorg. Chem.* **2015**, *54*, 2253–2263.
[54] A. C. Montenegro, V. T. Amorebieta, L. D. Slep, D. F. Martín, F. Roncaroli, D. H. Murgida, S. E. Bari, J. A. Olabe, *Angew. Chem. Int. Ed.* **2009**, *48*, 4213–4216.
[55] A. L. Speelman, C. J. White, B. Zhang, E. E. Alp, J. Zhao, M. Hu, C. Krebs, J. Penner-Hahn, N. Lehnert, *J. Am. Chem. Soc.* **2018**, *140*, 11341–11359.
[56] A. B. McQuarters, J. W. Kampf, E. E. Alp, M. Hu, J. Zhao, N. Lehnert, *Inorg. Chem.* **2017**, *56*, 10513–10528.
[57] F. Roncaroli, M. Videla, L. D. Slep, J. A. Olabe, *Coord. Chem. Rev.* **2007**, *251*, 1903–1930.
[58] C. Kupper, J. A. Rees, S. Dechert, S. DeBeer, F. Meyer, *J. Am. Chem. Soc.* **2016**, *138*, 7888–7898.
[59] T. S. Kurtikyan, V. A. Hayrapetyan, G. G. Martirosyan, R. K. Ghazaryan, A. V. Iretskii, H. Zhao, K. Pierloot, P. C. Ford, *Chem. Commun.* **2012**, *48*, 12088–12090.
[60] P. L. Piciulo, G. Rupprecht, W. R. Scheidt, *J. Am. Chem. Soc.* **1974**, *96*, 5293–5295.
[61] Z. N. Zahran, J. Lee, S. S. Alguindigue, M. A. Khan, G. B. Richter-Addo, *Dalton Trans.* **2004**, 44–50.
[62] Z. N. Zahran, M. J. Shaw, M. A. Khan, G. B. Richter-Addo, *Inorg. Chem.* **2006**, *45*, 2661–2668.
[63] M. Hoshino, S. Konishi, *Chem. Phys. Lett.* **1985**, *115*, 511–514.
[64] G. G. Martirosyan, A. S. Azizyan, T. S. Kurtikyan, P. C. Ford, *Inorg. Chem.* **2006**, *45*, 4079–4087.
[65] C.-H. Yu, Y. O. Su, *J. Electroanal. Chem.* **1994**, *368*, 323–327.
[66] B. O. Fernandez, I. M. Lorković, P. C. Ford, *Inorg. Chem.* **2003**, *42*, 2–4.
[67] P. C. Ford, I. M. Lorkovic, *Chem. Rev.* **2002**, *102*, 993–1018.
[68] F. Doctorovich, D. Bikiel, J. Pellegrino, S. A. Suárez, A. Larsen, M. A. Martí, *Coord. Chem. Rev.* **2011**, *255*, 2764–2784.
[69] I. Spasojević, I. Batinić-Haberle, I. Fridovich, *Nitric Oxide* **2000**, *4*, 526–533.
[70] W. R. Scheidt, A. Barabanschikov, J. W. Pavlik, N. J. Silvernail, J. T. Sage, *Inorg. Chem.* **2010**, *49*, 6240–6252.
[71] B. B. Wayland, L. W. Olson, Z. U. Siddiqui, *J. Am. Chem. Soc.* **1976**, *98*, 94–98.
[72] L. Chen, M. A. Khan, G. B. Richter-Addo, *Inorg. Chem.* **1998**, *37*, 533–540.
[73] N. Lehnert, W. R. Scheidt, M. W. Wolf, in *Nitrosyl Complexes in Inorganic Chemistry, Biochemistry and Medicine II* (Ed.: D.M.P. Mingos), Springer Berlin Heidelberg, Berlin, Heidelberg, **2014**, pp. 155–223.
[74] Ł. Orzeł, J. Polaczek, M. Procner, *J. Coord. Chem.* **2015**, *68*, 2971–2989.
[75] T. Diebold, M. Schappacher, B. Chevrier, R. Weiss, *J. Chem. Soc., Chem. Commun.* **1979**, 693–694.
[76] T. B. Demissie, J. Conradie, H. Vazquez-Lima, K. Ruud, A. Ghosh, *ACS Omega* **2018**, *3*, 10513–10516.
[77] P. Singh, A. K. Das, B. Sarkar, M. Niemeyer, F. Roncaroli, J. A. Olabe, J. Fiedler, S. Záliš, W. Kaim, *Inorg. Chem.* **2008**, *47*, 7106–7113.

[78] N. Xu, J. Lee, D. R. Powell, G. B. Richter-Addo, *Inorg. Chim. Acta* **2005**, *358*, 2855–2860.
[79] K. M. Kadish, V. A. Adamian, E. V. Caemelbecke, Z. Tan, P. Tagliatesta, P. Bianco, T. Boschi, G.-B. Yi, M. A. Khan, G. B. Richter-Addo, *Inorg. Chem.* **1996**, *35*, 1343–1348.
[80] K. M. Miranda, X. Bu, I. Lorković, P. C. Ford, *Inorg. Chem.* **1997**, *36*, 4838–4848.
[81] B. B. Wayland, L. W. Olson, *J. Am. Chem. Soc.* **1974**, *96*, 6037–6041.
[82] D. Lancon, K. M. Kadish, *J. Am. Chem. Soc.* **1983**, *105*, 5610–5617.
[83] L. W. Olson, D. Schaeper, D. Lancon, K. M. Kadish, *J. Am. Chem. Soc.* **1982**, *104*, 2042–2044.
[84] I. Kyu. Choi, Yanming. Liu, DiWei. Feng, K. Jung. Paeng, M. D. Ryan, *Inorg. Chem.* **1991**, *30*, 1832–1839.
[85] Z. Wei, M. D. Ryan, *Inorg. Chem.* **2010**, *49*, 6948–6954.
[86] Y. Liu, M. D. Ryan, *J. Electroanal. Chem.* **1994**, *368*, 209–219.
[87] Md. H. Rahman, M. D. Ryan, *Inorg. Chem.* **2017**, *56*, 3302–3309.
[88] E. G. Abucayon, R. L. Khade, D. R. Powell, Y. Zhang, G. B. Richter-Addo, *J. Am. Chem. Soc.* **2016**, *138*, 104–107.
[89] J. Lee, G. B. Richter-Addo, *J. Inorg. Biochem.* **2004**, *98*, 1247–1250.
[90] E. G. Abucayon, D. R. Powell, G. B. Richter-Addo, *J. Am. Chem. Soc.* **2017**, *139*, 9495–9498.
[91] E. G. Abucayon, R. L. Khade, D. R. Powell, M. J. Shaw, Y. Zhang, G. B. Richter-Addo, *Dalton Trans.* **2016**, *45*, 18259–18266.
[92] J. Pellegrino, S. E. Bari, D. E. Bikiel, F. Doctorovich, *J. Am. Chem. Soc.* **2010**, *132*, 989–995.
[93] R. G. Serres, C. A. Grapperhaus, E. Bothe, E. Bill, T. Weyhermüller, F. Neese, K. Wieghardt, *J. Am. Chem. Soc.* **2004**, *126*, 5138–5153.
[94] L. E. Goodrich, S. Roy, E. E. Alp, J. Zhao, M. Y. Hu, N. Lehnert, *Inorg. Chem.* **2013**, *52*, 7766–7780.
[95] J. Pellegrino, R. Hübner, F. Doctorovich, W. Kaim, *Chem. - Eur. J.* **2011**, *17*, 7868–7874.
[96] N. Kundakarla, S. Lindeman, Md. H. Rahman, M. D. Ryan, *Inorg. Chem.* **2016**, *55*, 2070–2075.
[97] R. Lin, P. J. Farmer, *J. Am. Chem. Soc.* **2000**, *122*, 2393–2394.
[98] C. E. Immoos, F. Sulc, P. J. Farmer, K. Czarnecki, D. F. Bocian, A. Levina, J. B. Aitken, R. S. Armstrong, P. A. Lay, *J. Am. Chem. Soc.* **2005**, *127*, 814–815.
[99] M. R. Kumar, D. Pervitsky, L. Chen, T. Poulos, S. Kundu, M. S. Hargrove, E. J. Rivera, A. Diaz, J. L. Colón, P. J. Farmer, *Biochemistry* **2009**, *48*, 5018–5025.
[100] W. Robert. Scheidt, J. L. Hoard, *J. Am. Chem. Soc.* **1973**, *95*, 8281–8288.
[101] E. Fujita, C. K. Chang, J. Fajer, *J. Am. Chem. Soc.* **1985**, *107*, 7665–7669.
[102] A. D. Kini, J. Washington, C. P. Kubiak, B. H. Morimoto, *Inorg. Chem.* **1996**, *35*, 6904–6906.
[103] S.-H. Cheng, Y. O. Su, *Inorg. Chem.* **1994**, *33*, 5847–5854.
[104] G. B. Richter-Addo, S. J. Hodge, G.-B. Yi, M. A. Khan, T. Ma, E. Van Caemelbecke, N. Guo, K. M. Kadish, *Inorg. Chem.* **1996**, *35*, 6530–6538.
[105] K. M. Kadish, Z. Ou, X. Tan, T. Boschi, D. Monti, V. Fares, P. Tagliatesta, *J. Chem. Soc., Dalton Trans.* **1999**, 1595–1602.
[106] C.-H. Chuang, W.-F. Liaw, C.-H. Hung, *Angew. Chem.* **2016**, *55*, 5190–5194.
[107] A. Mazzeo, J. Pellegrino, F. Doctorovich, *J. Am. Chem. Soc.* **2019**, *141*, 18521–18530.
[108] H. Seki, M. Hoshino, S. Kounose, *J. Chem. Soc., Faraday Trans.* **1996**, *92*, 2579–2583.
[109] C. E. McKenna, W. G. Gutheil, W. Song, *Biochim. Biophys. Acta, Gen. Subj.* **1991**, *1075*, 109–117.
[110] M. H. Barley, T. J. Meyer, *J. Am. Chem. Soc.* **1986**, *108*, 5876–5885.
[111] V. Shafirovich, S. V. Lymar, *Proc. Natl. Acad. Sci. U.S.A.* **2002**, *99*, 7340–7345.
[112] J. J. Warren, T. A. Tronic, J. M. Mayer, *Chem. Rev.* **2010**, *110*, 6961–7001.
[113] Y. Fang, Y. G. Gorbunova, P. Chen, X. Jiang, M. Manowong, A. A. Sinelshchikova, Y. Yu. Enakieva, A. G. Martynov, A. Yu. Tsivadze, A. Bessmertnykh-Lemeune, C. Stern, R. Guilard, K. M. Kadish, *Inorg. Chem.* **2015**, *54*, 3501–3512.
[114] B. H. Solis, A. G. Maher, D. K. Dogutan, D. G. Nocera, S. Hammes-Schiffer, *Proc. Natl. Acad. Sci. U.S.A.* **2016**, *113*, 485–492.
[115] F. Sulc, E. Fleischer, P. J. Farmer, D. Ma, G. N. La Mar, *JBIC, J. Biol. Inorg. Chem.* **2003**, *8*, 348–352.
[116] Md. H. Rahman, Y. Liu, M. D. Ryan, *Inorg. Chem.* **2019**, *58*, 13788–13795.
[117] N. O. Codesido, T. Weyhermüller, J. A. Olabe, L. D. Slep, *Inorg. Chem.* **2014**, *53*, 981–997.
[118] S. Kelly, D. Lancon, K. M. Kadish, *Inorg. Chem.* **1984**, *23*, 1451–1458.
[119] B. B. Wayland, J. V. Minkiewicz, M. E. Abd-Elmageed, *J. Am. Chem. Soc.* **1974**, *96*, 2795–2801.
[120] F. Roncaroli, R. van Eldik, *J. Am. Chem. Soc.* **2006**, *128*, 8042–8053.
[121] K. M. Kadish, X. H. Mu, X. Q. Lin, *Inorg. Chem.* **1988**, *27*, 1489–1492.
[122] M. Tang, Y. Yang, S. Zhang, J. Chen, J. Zhang, Z. Zhou, Q. Liu, *Inorg. Chem.* **2018**, *57*, 277–287.
[123] M. Wolak, A. Zahl, T. Schneppensieper, G. Stochel, R. van Eldik, *J. Am. Chem. Soc.* **2001**, *123*, 9780–9791.
[124] A. Franke, F. Roncaroli, R. van Eldik, *Eur. J. Inorg. Chem.* **2007**, *2007*, 773–798.
[125] H. A. Hassanin, L. Hannibal, D. W. Jacobsen, K. L. Brown, H. M. Marques, N. E. Brasch, *Dalton Trans.* **2008**, 424–433.
[126] M. A. Rhine, A. V. Rodrigues, R. J. B. Urbauer, J. L. Urbauer, T. L. Stemmler, T. C. Harrop, *J. Am. Chem. Soc.* **2014**, *136*, 12560–12563.
[127] M. R. Walter, S. P. Dzul, A. V. Rodrigues, T. L. Stemmler, J. Telser, J. Conradie, A. Ghosh, T. C. Harrop, *J. Am. Chem. Soc.* **2016**, *138*, 12459–12471.
[128] B. C. Sanders, M. A. Rhine, T. C. Harrop, in *Molecular Design in Inorganic Biochemistry* (Ed.: D. Rabinovich), Springer, Berlin, Heidelberg, **2014**, pp. 57–88.
[129] J. Conradie, A. Ghosh, *J. Phys. Chem. B* **2016**, *120*, 4972–4979.
[130] Y. Guo, J. R. Stroka, B. Kandemir, C. E. Dickerson, K. L. Bren, *J. Am. Chem. Soc.* **2018**, *140*, 16888–16892.
[131] A. Mazzeo, S. Santalla, C. Gaviglio, F. Doctorovich, J. Pellegrino, *Inorg. Chim. Acta* **2021**, *517*, 119950.
[132] C. M. Gallego, A. Mazzeo, P. Vargas, S. Suárez, J. Pellegrino, F. Doctorovich, *Chem. Sci.* **2021**, *12*, 104010–10425.
[133] D. M. P. Mingos, in *Nitrosyl Complexes in Inorganic Chemistry, Biochemistry and Medicine I* (Ed.: D.M.P. Mingos), Springer, Berlin, Heidelberg, **2014**, pp. 1–44.
[134] G. Monsch, P. Klüfers, *Angew. Chem. Int. Ed.* **2019**, *58*, 8566–8571.

Entry for the Table of Contents

Insert graphic for Table of Contents here.

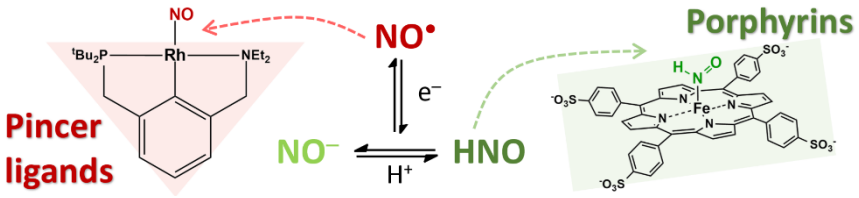

Insert text for Table of Contents here.

This review explores the existing literature on nitrosyl and nitroxyl complexes with pincer and porphyrin ligands, both of which have been important topics in our research group. The organometallic reactivity of pincer nitrosyls is presented, along with synthetic strategies and characterization methods. Biologically relevant nitroxyl porphyrin complexes are also described, focusing on their characterization and discussing the factors influencing their stability.

Institute and/or researcher Twitter usernames:

INQUIMAE Research Institute: @Inquimae1

Fabio Doctorovich: @DoctFabio

Juan Pellegrino: @juan_pell

Agostina Mazzeo: @agoszz

Cecilia M. Gallego: @cecisnp